AN INTEGRATED SHIP RE-DESIGN/MODIFICATION STRATEGY

(DOI No: 10.3940/rina.ijme.2019.a1.509)

A K P Patel Department of Naval Architecture and Offshore Engineering, AMET University, Chennai, India and **R Sharma** Design and Simulation Laboratory, Department of Ocean Engineering, Indian Institute of Technology Madras, Chennai, India

SUMMARY

Herein, we present an integrated ship re-design/modification strategy that integrates the 'Computer-Aided Design (CAD)' and 'Computational Fluid Dynamics (CFD)' to modify the ship hull form for better performance in resistance. We assume a modular design and the ship hull form modification focuses on the forward module (e.g. bulbous bow) and aft module (e.g. stern bulb) only. The ship hull form CAD model is implemented with NAPA^{*TM} and CFD model is implemented with Shipflow^{**TM}. The basic ship hull form parameters are not changed and the modifications in some of the technical parameters because of re-designed bulbous bow and stern bulb are kept at very minimum. The bulbous bow is re-designed by extending an earlier method (Sharma and Sha (2005b)) and stern bulb parameters for re-design are computed from the experience gained from literature survey. The re-designed hull form is modeled in CAD and is integrated and analyzed with Shipflow^{**TM}. The CAD and CFD integrated model is validated and verified with the ITTC approved recommendations and guidelines. The proposed numerical methodology is implemented on the ship hull form modification of a benchmark ship, i.e. KRISO container ship (KCS). The presented results show that the modified ship hull form of KCS - with only bow and stern modifications - using the present strategy, results into resistance and propulsive improvement.

NOMENCLATURE

x, y, z	Directions in the rectilinear coordinate system,
g	Gravitational acceleration,
k	Wave number,
p	Pressure force,
T or H	Mean draft of the ship,
FP	Forward perpendicular,
ϕ	Velocity potential,
ρ	Fluid density,
η	Instantaneous wave height,
μ	Dynamic viscosity,
ν	Kinematic viscosity,
$\forall_{PR}$	Protruding volume of bulb,
$\forall_{BTOT}$	Total bulb volume,
$\forall_{WL}$	Displacement volume of ship at the L_{LWL},
$\forall_{SB}$	Protruding volume of stern bulb,
ς	Ship's beam/length ratio,
σ_{ij}	Total stress,
δ_{ij}	Kronecker delta,
S_{ij}	Strain rate,
μ_T	Turbulent viscosity,
ν_T	Turbulent kinematic viscosity,
k	Turbulent kinetic energy,
δ^*_{SN}	Simulation numerical error,
δ_{SM}	Modeling error,
A_{BL}	Area of bow in longitudinal direction,
A_{BT}, and $A_{BT}(x)$	Transverse cross-sectional area of the bulb at FP,
A_{MS}	Mid-ship sectional area,
A_{SBT}	Transverse cross-sectional area of the stern bulb at AP,
B or B_{MS}	Ship beam at the mid-ship,
B_B	Maximum breadth of bulb area A_{BT},
B_{SB}	Maximum breadth of stern bulb area A_{SBT},
C_{ABL}	Longitudinal or lateral parameter for the bulb,
C_{ABT}	Cross section parameter for the bulb,
C_{BB}	Breadth parameter for the bulb,
C_{CG}	Volumetric distributional parameter for the bulb,
C_F	Frictional resistance coefficient,
C_G	Correction factor, and
C_{LPR}	Length parameter for the bulb,
C_P	Pressure coefficient,
C_T	Total resistance coefficient,
C_W	Wave making resistance coefficient,
C_{ZB}	Depth parameter for the bulb,
$C_{\forall TOT}$	Protruding volume parameter for the bulb,
F_n	Froude number,
F_X	X-component of the total hydrodynamic force,
H_B	Height of the bulb measured at A_{BT},
H_{SB}	Height at which the A_{SBT} and V_{SB} are limited,
H_W	Instantaneous wave height,
L_{PP}	Length between perpendiculars,
L_{PR}	Protruding length of bulb,
L_{LWL} or L	Length on load water line,

LCG_B	Longitudinal center of gravity of the bulb,
p_a	Atmospheric pressure,
P_G	Estimated order of accuracy,
P_i	Group of ship offsets,
R_G	Convergence ratio,
R_i	Body force intensity in x, y, z directions,
S_C	Corrected simulation,
U_i	Component of instantaneous velocity,
$U_{S_C N}$	Uncertainty in the error estimate,
U_{SN}	Numerical uncertainty,
V_A	Speed of advance,
V_S	Design speed of the ship (e.g. KCS),
V_z	Vertical component of the resultant velocity,
w_n	Nominal wake,
Z_B	Height of the foremost point above keel line on the bulb at FP,
Z_{SB}	Height of the foremost point above keel line on the stern bulb at station 1, and
$u_i^{"}$	Fluctuating velocity component.

1. INTRODUCTION

Engineering structures - ships and floating structures - are getting more and more complex with time because of the requirements of efficiency, economy, safety, comfort and aiming for lower carbon footprint. Furthermore, the demands of competition are making modern engineering designs increasingly more complicated, e.g. pressing demands of economies of scale, higher speed, lower motions, operational ability in adverse weather conditions, energy efficiency, clean environment, and advancements in material science and technologies. The economies of scale and demands of efficient transportation are pushing the ship size and speed to higher values with passing of each one of the decades starting from late 20th century till date, e.g. Container ship: Mærsk Mc-Kinney Møller ship, speed = 23 knots, size = 18 270 TEU containers/194 153 DWT; Oil tanker ship: TI-class supertanker, speed = 16.5 knots, size 441 585 DWT; Ocean liner: RMS Queen Mary 2, speed = 30 knots, size = 148 528 GT; and Bulk carrier ship: MS Berge Stahl, speed = 13.5 knots, size = 364 767 DWT. Also, the ships and floating structures serve a wide variety of objectives, e.g. transporting cargo and passengers, exploration/production/storage of oil/gas/minerals, coastal protection and surveillance, and military defense, etc. It is interesting to note here that the ships and floating structures are one of largest man made and complex engineering structures whose design and analysis time runs in months and production may take anywhere between months to years. This scenario demands the design and development of new products within a shorter lead time. Additionally, the ships are customized, capital intensive and long service life products.

A design's performance can change with time depending upon the prevailing fuel oil prices, e.g. the optimum speed of the ship will rise in low fuel oil price period and fall in high fuel oil price period. In general, the fuel oil prices have shown highly non-linear trends with periods of high and low prices. However, normally each one of the passing decades has shown a higher averaged crude oil price than the preceding decade. From the carbon foot print and energy efficiency points of view, the performance of a ship in terms of resistance and power becomes critical because a lower resistance and power can improve the ship's operating economics. After signing ship building contract, the shipyard's design office prefers a detailed performance analysis of ship resistance and propulsion model tests aimed at resistance measurements, determination of ship speed, propeller rotational speed and propulsion engine power for the designed ship, and the possibility of hull form improvements. Normally, the range of ship hull modifications is limited because of the involvement of high cost and time. However, assuming that the ship design is based upon 'modular concept' and/or ship is open for conversion possibilities, then the numerical methods (i.e. computational fluid dynamics) can be used to create the alternate designs that are more efficient in resistance and propulsive power and with minimum modifications on the overall design.

In the field of naval architecture and ocean engineering, design and analysis cannot be conceived as separate entities and design of new ships is based on structural analysis, hydrodynamic analysis and manufacturing analysis. The process of design starts with 'computer aided design (CAD)' systems and follows the CAD model with other analyses, e.g. structural analysis with 'finite element analysis (FEA)', hydrodynamic analysis with 'computational fluid dynamics (CFD)' and manufacturing analysis with plate development and thermal simulation via FEA.

The basic problem in the integration of CAD, FEM and CFD is: All of these procedures originated at a different time span. The FEA and CFD preceded CAD and the rich geometric forms (i.e. shape functions, and basis function, etc.) prevalent in modern CAD systems came only during 1975-1990 and found popularity in the industrial system around 2000. The FEA started around 1950-60 and major foundations including detailed mathematical understanding were laid during 1970-1980, and since 1980 it has been extremely popular in engineering analysis and design. Similarly, the CFD started around 1960s, gained deeper and meaningful understanding in 1980s, and with NASA's successful three-dimensional coding of the Navier–Stokes, numerous commercial software packages later became available for industrial and academic usages.

It can be noted here that though a single CAD definition for CAD to FEA to CFD to manufacturing simulation is highly desired to achieve an integrated design and analysis cycle, it is still at the research stage only and likely to take some more time before it can be incorporated in industrial designs and analyses. A ship is represented by its offset and the CAD model is generated from the given offset with desired levels of continuity and differentiability. This CAD model is used to generate the meshes/grids in FEA/CFD. A change in the control points of the CAD model will change ship geometry and this change can be studied with FEA/CFD systems for structural and hydrodynamic features. Of course for the design and development of new ships this needs to be changed. Now, the scientific and technical objectives in the present research environment are to create a new computational framework which is suitable for CAD, FEA, and CFD analyses.

It is important to note here that the naval architecture and offshore structure communities have been one of the earliest users of computers in design and manufacturing. In fact they have played a significant role in developing the foundations of the spline functions, B-spline and non-uniform B-spline, etc., for more details see Nowacki and Bloor (1995), Patrikalakis and Maekawa (2002), and Sapidis (1987). However, even though the ships and offshore structures are routinely modeled in CAD systems that are based upon the NURBS, etc., the use of NURBS in FEM and CFD (with the exception of use in the 'Boundary Element Method (BEM))' have not been attempted even by the naval architecture and offshore structure communities.

An efficient analysis suitable model is difficult to generate and it involves couple of time consuming and preparatory steps. In the field of naval architecture and ocean engineering, the benefits of design optimization have been largely unavailable because for the efficient shape optimization the CAD geometry-to-mesh conversion needs to be automatic, differentiable and tightly integrated with the solver and optimizer, e.g. Reynolds-averaged Navier-Stokes (RANS) solver. There are two possible approaches for integration of the design through analysis process:

- *Approach 1:* This deals with the software to software integration and offers only partial integration and basically implies that the output of one software is input to the next or other software, e.g. output of NAPA^{*TM} is input to Shipflow^{**TM}.

- *Approach 2:* This deals with the full integration and implies that the functional and geometric definitions are common in CAD, CFD and FEM, e.g. 'Iso-geometric Analysis (IGA)'. E.g. in IGA the works of Hughes *et al*. (2005) and Cottrell *et al*. (2009) have shown that it preserves the geometry at all levels of refinement and that detailed features can be retained without excessive mesh refinement, in contrast with traditional finite element analysis. The IGA leads to superior accuracy in the FEA on a degree-of-freedom basis and impressive results of significantly increased robustness in vibration and wave propagation analysis. However, the IGA is at the research stages and yet to attain its full potential applications.

We focus on the '*Approach 1*' and use the CAD definition of NAPA^{*TM} to generate the grids that are used in Shipflow^{**TM} and in this process we integrate the CAD and CFD for re-design application.

Our focus is on 'ship hull form modification' to improve a chosen performance parameter. A ship can be modified at the following stages:

Stage 1 – Contract signing stage: After signing ship building contract, the shipyard's design office can modify the ship's design. Although, modifications at this stage are possible, they are limited in-general because of the involvement of high cost and time and un-willingness of shipyard/s.

Stage 2 – Conversion stage: A ship can be converted into some other type of ship during its lifecycle. At this stage, the ship can be modified and the opportunities for ship hull form modification are larger, e.g. the forward and aft parts of ship can be modified along with the fairing of ship lines.

Though, in this paper the main focus is on 'Stage 2' as mentioned above, but depending upon the willingness of shipyard the approach can be implemented in 'Stage 1' also. The aim is to design and develop a numerical methodology that integrates the CAD and CFD to modify the ship hull form for better performance in resistance, propulsion and hence better energy efficiency. However, the focus is only on modification of the forward and aft parts of ship and not on the fairing of ship lines. It is only because of: 1) it is easy to modify the ship in aft and forward bodies, 2) forward body affects the resistance most and 3) aft body affects the propulsion and power.

Herein, the forward part of ship is modified first and then the ship with modified forward part is modified further in the aft part. The ship hull form CAD model is implemented with NAPA^{*TM} and CFD model is implemented with Shipflow^{**TM}. The basic ship hull form parameters are not changed and the modifications in some of the technical parameters because of re-designed bulbous bow and stern bulb are kept at very minimum. The bulbous bow is re-designed by extending an earlier method (Sharma and Sha (2005b)) and stern bulb parameters for re-design are computed from the experience gained from literature survey. The CAD and CFD integrated model is validated and verified with the ITTC approved recommendations and guidelines. The proposed numerical methodology is implemented on the ship hull form modification of an existing ship in service, i.e. Korean container ship (KCS). A through and detailed

treatment of the theory and examples reported in present paper can be found in the recent thesis of Patel (2016).

The remaining of present paper is organized: Section 2 discusses the re-design strategy including the design parameters and methodology of the re-design and modification; Section 3 presents the CAD modeling of ship with NAPA*TM and its integration with the CFD analysis (i.e. with Shipflow**TM); Section 4 discusses the CFD analysis, basic governing equations and 'verification and validation (V&V)' strategy; Section 5 presents the numerical example and discussion; and Section 6 concludes the paper with recommendations for future work.

1.1. BRIEF REVIEW OF LITERATURE

Although the idea of bulb is integral to the modern ship design, the research on design methods for bulbous bow is rare. To the best of authors' knowledge except Kracht (1978), Yim (1980) and Sharma and Sha (2005a and 2005b) no other research results are available in the public domain that present a design method for bulbous bow for ships. And, in these works the limitations are the following:

- The results are presented for the narrow ranges, e.g. Sharma and Sha (2005a) - the C_B ranges from 0.5 to 0.525 and F_n ranges from 0.17 -0.385; Sharma and Sha (2005b) - the C_B ranges from 0.675 to 0.725 and F_n ranges from 0.20 -0.26; Kracht (1978) - only one C_B is considered; and Yim (1980) gives results for an optimum spherical bulbous bow which is difficult to fair in both U and V shaped fore-bodies and also has high production complexity as the sphere is a non-developable surface.
- The effects of production constraints on ship hull form design with bulbous bow are not considered.
- The integration of the CAD model with design and hydrodynamic analysis is not considered.

With the advancements in CAD and CFD software solution systems, significant research efforts started in the direction of integration of CAD and CFD and its application in ship hull form design and analysis, e.g. Tahara *et al*. (2008), Campana *et al*. (2009), Kim and Yang (2010), Nowacki (2010), Papanikolaou (2010), Serani *et al*. (2014), Kostas *et al*. (2015), Park *et al*. (2015), Chen *et al*. (2016), Huang and Yang (2016), Yang and Huang (2016), and the references therein. Although, the existing researches have focused upon the integration of CAD and CFD and utilized this integration to modify the ship hull form for improvements in resistance and power etc., none of them have reported any study about how to design the bulbous bow for a particular ship to start with? All of them start with a design and assume that the bulbous bow design is available to them.

Additionally, the existing researches have the following limitations:

- Production aspects have not explored and it is not known how the sectional shapes are to be designed to keep the production cost low?
- The results are presented for a specific ship and, although the approach can be the same for other ships, the automatic hull modification procedures proposed have limited applicability, e.g. they are applicable to fine form ships of low C_B.
- A modification is needed to ensure that the gains in resistance are not lost in power. Also, it is desirable to investigate the forward modification along with the aft modifications to ensure compatibility between resistance, power, maneuverability and space requirements. This aspect has not been explored in the existing ship hull form modification process.
- The primary aim of a designer is to generate alternative ship designs that can cater to the needs of different owner and order placing agencies. This aspect is ignored in the current researches.
- A design process is implemented in steps and because of this it is important to investigate a step-wise design approach. Furthermore, the design of a bulbous bow must be related to the basic ship parameters. Otherwise, the results would be difficult to reproduce across a range of applications.

In this paper, we address the above mentioned limitations of the existing researches. Also, we report a comprehensive comparison of the current research with previous researches later in Table 10 and show that our present approach and results advance the area of ship design.

1.2. RESEARCH CONTRIBUTION

Our important contribution is a design method for bulbous bows for ships in the range C_B = 0.650 - 0.725 and F_n = 0.260 - 0.300 along with a detailed CFD driven approach for the hydrodynamic analysis integrated with CAD. Additionally, we note the following features:

- We present an integrated ship re-design/modification strategy and this approach is applicable to different types of ships in the ranges mentioned above. It can be noted here that these ranges cover a large group of commercial ships.
- The results presented in Figures. 5 to 7 are applicable to the design of ships with bulbous bows and can be utilized by small and medium shipyards that do not have access to expensive 'Computational Fluid Dynamic (CFD)' software solution systems. These results can be used by any shipyard or ship designer.
- For the sake of completeness and reproducibility, we report some important lines drawings of the design alternatives that have been developed. Any naval architect can check the drawings and confirm their applicability.

- Production aspects have been explored and section shapes have been designed to keep the production cost low. This is explained in detail in Section 2.3. Also, the design process is detailed with steps. These will allow others to reproduce and check the authenticity of the developed designs.
- In Section 2.4, we present a discussion on 'Aft modifications' that is unique and expected to open the next approach to the design of a ship's aft sections.
- Each of the sections is detailed and contains full details of the implementation of the proposed design process, the approach to the implementation, and a reasoned explanation of its uses. Each section also lists what can be done next, i.e. scope for further research. This will help and motivate further research into next level approaches to ship re-design and modification.
- For the first time, we show that in the proposed ship re-design/modification approach, the gains in resistance will not be lost in power. This is analyzed in detail in Section 5.5.

2. RE-DESIGN STRATEGY

Herein, we focus on ship re-design/modification by considering only resistance and power performance of the ship as the main objectives.

2.1. MODULAR DESCRIPTION OF THE DESIGN

A ship can be re-designed or modified from one end (aft end) to another end (forward end), in different ways, e.g. whole ship or only a part of it. It is neither practical nor economical to re-design or modify the entire ship because of the prohibitively high cost involved in cutting the ship and incorporating all the desired changes in production. An easier option is to cut the ship at any of the stations close to either the 'Forward Peak Bulkhead (FPB)' or 'Aft Peak Bulkhead (APB)' or both and then focus either on the forward part in forward of chosen station or on the aft part in aft of chosen station in aft APB, or on the both, respectively. It is important that we select stations that are closest to the APB and FPB. This approach is simple and economical to be implemented in the ship production processes and this is applicable at the all stages of ship design and production. However, this approach offers only limited advantages because it does not alter the principal dimensions likes 'Breadth (B_{MS})' and 'Draft (H)' and allows only minor changes in 'Length on the Load Water Line (L_{LWL})', 'Block Coefficient (C_B)' and 'Displacement ($\forall_{WL}$), etc. Since, the changes are limited the gains are also limited. Also, we note that if the basic principal dimensions are selected wrongly in a design then it is difficult to achieve reasonable gains through any of the re-design and modification strategies. We assume that the basic principal dimensions are fine and assuming that we focus on re-design and modification of the forward part and aft part to achieve reasonable and meaningful gains in resistance. Additionally, we ensure that the gains in resistance are not lost in power.

Since, we focus on re-design and modification of the forward and aft parts, we assume the ship to be of a modular design. In modular design, a ship is conceived of five modularized hull parts or zones: 'Aft Body Module (ABM)', 'Mid Body Modules (MBM)', 'Fore Body Module (FBM)', 'Transition Module of merging of Fore Body with Mid Body (TMFBMB)' and 'Transition Module of merging of Aft Body with Mid Body (TMABMB)', for details see Misra *et al*. (2002), Sha *et al*. (2004), Sharma and Sha (2007), Misra (2015). A modular design offers the following unique and distinct advantages:

- The change in a specific module affects: transition zone and/or that module. E.g. if the forward module is changed then only the forward zone and transition zone (i.e. transition zone of merging of fore body with mid body) will be modified and there will not be any effect on the other modules (i.e. aft body, mid body, and transition zone of merging of aft body with mid body). It implies that there will be limited fairing requirements restricted to the changed zones. This is advantageous for both the design and production processes. As the changes to be done in process of re-design/modification are only limited to a selected 'zone' in the ship with modular design configuration, this allows the designer to convince the ship owner regarding re-design/modification as the changes will be efficient in terms of cost and time. The same idea is efficiently implementable in ship conversion because in the conversion process the ship owners normally prefer the limited modifications either in the forward or aft or both, if they can improve the resistance and delivered power?
- Newer designs catering to different set of requirements can be generated by different permutations and combinations of different modules. E.g. even with the fixed ABM, MBM, and TMABMB, we can generate new designs offering varying performances in terms of resistance and power by just changing the FBM and TMFBMB. This will result into designs with different bulbous bows.
- The changes in geometric shapes are limited only to certain modules and the maximum size of the design remains unchanged in geometric shapes. This can offer significant advantages in terms of grid generation because grids can also be stored for specific parts and the stored grids can be used again in the loop without any need for regenerating the grid for a part that is not changed. This idea is possible, feasible and expected to reduce the computational time significantly. However, in the

present work, we have not implemented this. This is to be investigated in future.

2.2 SELECTION OF THE SHIP TYPE/MODEL AND PARAMETERS

We study a container ship to demonstrate our proposed re-design/modification strategy, i.e. the 'KRISO container ship (KCS)' and the principle particulars of KCS are listed in Table 1. The CAD model of KCS is shown in Fig. 1. In case of the displacement vessels, which operate in range of $F_n = 0.20 - 0.28$, wave making component of the resistance is predominant at higher speed and that is mainly affected by the forward and aft part of ship. Figures. 2a and 2b show the variation of co-efficient of total resistance (C_T) and wave-making resistance (C_W) with F_n for the KCS Initial Design (ID) and these are the computed values using the CAD model with the Shipflow[**TM] software solution system. The oscillations in Figure. 2 are primarily because of the limitations of computations and plotting as they are curtailed at certain iterations and because of this it is difficult to capture the exact pattern without oscillations. Furthermore, the waves generated by a moving ship are affected by her geometry (i.e. volume, shape and their distribution) and speed. The energy given by the ship for creating waves is transferred to water through three parts: Middle, bow and stern parts. Now, these three wave systems interact with each other and the resulting waves are responsible for the wave making resistance. Depending upon the speed and geometry these three waves get superimposed differently at each of the speeds and these results into the slightly non-linear behavior in the wave making resistance. This emphasizes the need of reducing wave-making component at higher speed for the economically efficient design. Again for the KCS ID, Figure. 3 shows the variation of co-efficient of frictional resistance (C_F) with F_n, and we observe that there is a no significant change in the C_F even at higher F_n.

Table 1: New design values of bulbous bow, initial values for KCS's bulb and the computed dimensions of bulb from of coefficients.

Technical parameters of the KCS - ID								
Parameter			Value					
L_{PP}			230.00 m					
B			32.200 m					
T, D			10.80 m, 16.0 m					
C_B, F_n, V_s			0.65, 0.255, 24 knots					
Bulb parameters								
Design parameters for the bulb modification			Bulb dimensions derived from design parameters					
Design parameters	Initial value	New value	Parameters	Initial value	Computed parameters from Figs. 5 to 7	Design alternative D1	Design alternative D2	Design alternative D3
C_{BB}	0.14800	0.1830	B_B (m)	4.7630	5.89600	5.900	6.20	5.940
C_{LPR}	0.03011	0.0475	L_{PR} (m)	7.0000	11.0000	10.13	10.0	10.25
C_{ZB}	0.50420	0.8000	Z_B (m)	5.4450	8.64000	1.390	5.00	8.330
C_{ABT}	0.08510	0.1170	A_{BT} (m^2)	29.129	40.2500	35.12	38.0	34.94
C_{ABL}	0.13500	0.1570	A_{BL} (m^2)	46.330	53.7710	60.00	53.8	51.34
$C_{\nabla TOT}$	-	0.0130	$\forall_{BTOT}$ (m^3)	-	676.432	-	-	-
C_{CG}	0.18000	0.2800	LCG_B	2.8300	4.40000	-	-	-

Figure 1: CAD drawing of the KCS ID using NAPA*TM.

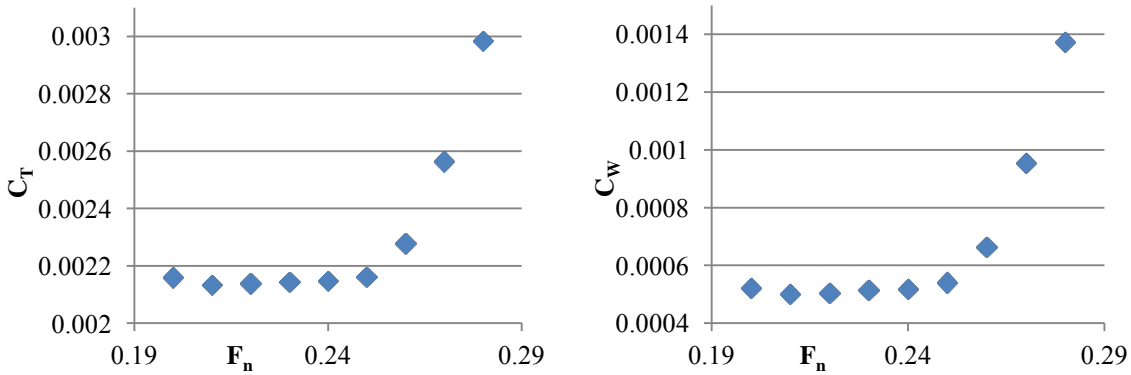

(a) Variation of C_T with F_n (b) Variation of C_W with F_n.

Figure 2: Variation of the C_T and C_W with F_n for the KCS ID.

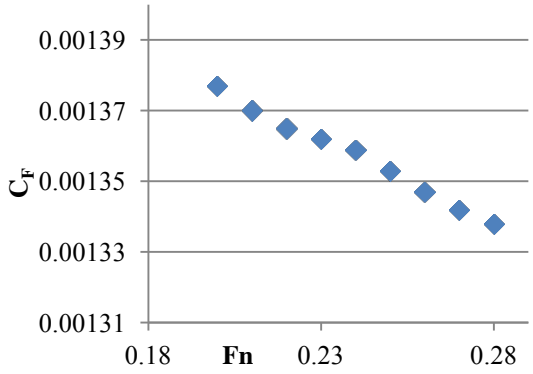

Figure 3: Variation of the C_F with F_n for the KCS ID.

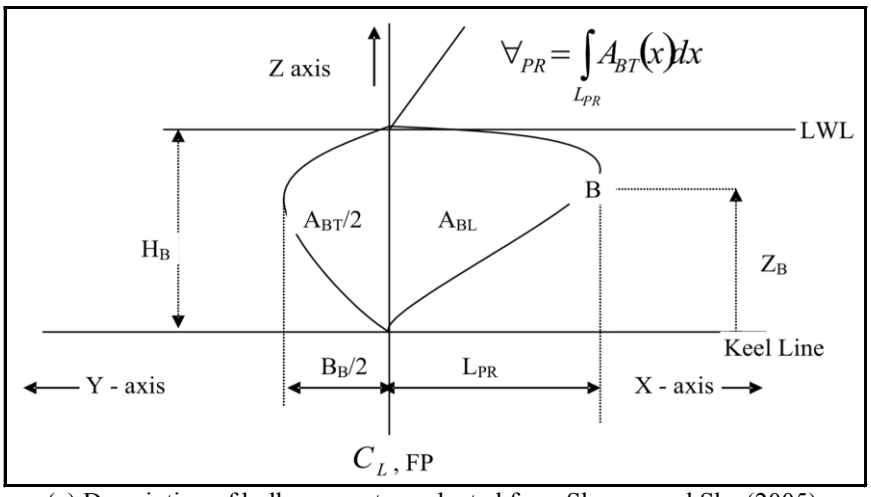

(a) Description of bulb parameters adapted from Sharma and Sha (2005).

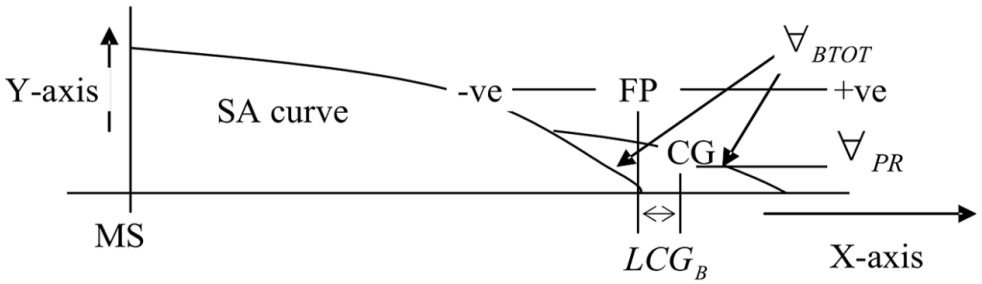

(b) Description of bulb parameter LCG_B adapted from Sharma and Sha (2005).

Figure 4: Description of bulb parameters.

In the present study, design modifications are limited to the concept design phase, where ship hydrodynamic performance (resistance) is studied closely under certain conditions. E.g. evolution in container ship size, accrued fuel prizes, IMO regulations, classification rules, etc., are some of the few design constraints that can be considered at the concept design phase. However, we restrict the design modifications to the forward and aft parts of the ship only, i.e. bow and stern.

2.3 SHIP FORWARD MODIFICATIONS – DERIVATION OF BULBOUS BOW DESIGN PARAMETERS

In theoretical accordance with Kracht (1978) and Sharma and Sha (2005b), three linear and four non-linear parameters are sufficient to describe the bulb form. These seven parameters are non-dimensionalized with respect to the ship particulars and are shown in Figure. 4. Also, the ship's forward flow entrance is modified to incorporate the effective modifications in the existing bulb design. These seven design parameters are:

- C_{BB} is the breadth parameter and defined as $C_{BB} = B_B / B_{MS}$,
- C_{LPR} is the length parameter and defined as $C_{LPR} = L_{PR} / L_{LWL}$,
- C_{ZB} is the depth parameter and defined as $C_{ZB} = Z_B / H$,
- C_{ABT} is the cross section parameter and defined as $C_{ABT} = A_{BT} / A_{MS}$,
- C_{ABL} is the lateral parameter and defined as $C_{ABL} = A_{BL} / A_{MS}$,

- $C_{\forall PR}$ is the volumetric parameter and defined in percentage as $C_{\forall PR} = \forall_{LR} / \forall_{WL}$*100. The volume $\forall_{PR}$ is distributed forward of FP. The total volume $\forall_{BTOT}$ is defined as the sum of $\forall_{PR}$ and fairing volume required aft of FP to fair the bulb in the ship (in both additive and implicit bulbs). In the same manner another volumetric coefficient is defined: $C_{\forall TOT} = \forall_{BTOT} / \forall_{WL}$, and
- C_{CG} is the volumetric distributional parameter and defined as $C_{CG} = LCG_B / (L_{LWL} \cdot F_n^2)$.

Primarily, an important difference between the ship-wave problem and other thin-body hydrodynamic problems (i.e. airfoil and cavitation problems) is the existence and effects of the free surface. In theoretical accordance with the other theories (i.e. linear airfoil and cavitation theories) the basic assumption in the theory of Michell (1898) is that the ship is thin and flow perturbations due to the ship are related only to the ship's beam/length ratio (i.e. $\varsigma = B_{MS} / L_{LWL}$). This is particularly not true for $\varsigma > 0.1$ and this effect of breadth-length ratio on the resistance is known as '*sheltering effect*', Yim (1974). For the higher values of ς, this effect is complicated by mutual interferences of the thinness parameter ς, the wave number *k*, and the boundary layer thickness. As was done in Sharma and Sha (2005b), herein, the first six parameters are derived by re-correlation with statistical analysis and the seventh parameter by re-analysis of an approximate linear theory with sheltering effect for resistance estimation. The analysis has been done for maximum and relatively constant (i.e. 0.35 - 0.45, discrete maximum error = 10%) and in a narrow range of ship particulars (i.e. C_B = 0.650 - 0.725, C_{WL} = 0.75 - 0.85, C_M = 0.80 - 0.99, C_{PE} = 0.60 - 0.75, L_{LWL}/B = 5.2 - 7.55, B/H = 2.15 - 3.15, L_E/B = 2.05 - 3.8, and Fn = 0.26 - 0.30). The results have been presented for the range of C_B = 0.650, 0.675, 0.70 and 0.725, and F_n = 0.26 - 0.30. These results are shown in Figures. 5a, 5b, 5c, 5d, 6a, 6b, and 6c. Similar to Sharma and Sha (2005), herein, the seventh parameter (i.e. $C_{CG} = LCG_B / \left(L_{WL} . Fn^2\right)$) is derived by re-analysis of an approximate linear theory with sheltering effect for resistance estimation. To approximate the solution function for optimum location it is assumed that the optimum location is a function of only $H/L_{LWL}, B_{MS}/L_{LWL}$, and z/H_1 in the range of C_B = 0.650 - 0.725, hence neglecting the complexities. Assuming a point doublet located near the bow stem at a typical depth of z/H_1 = 0.75 - 0.85 (i.e. for C_B = 0.650 - 0.725, and Fn = 0.2 - 0.26 which is a fair approximation), the approximate optimum location of the bulb is computed. In general, the waterlines of a ship are not similar to waterlines of a sine ship, cosine ship or parabolic ship. However, in specific cases a multivariate function (i.e. a function of sine, cosine and parabolic distributions) fitting the waterlines can be assumed, Yim (1980). The optimum locations (i.e. $C_{CG} = LCG_B / \left(L_{WL} . Fn^2\right)$) are shown in Figures. 6d, 7a, 7b and 7c.

We note here that the design parameters of bulb are derived through an analysis and this analysis results into computation of the parameters without the considerations of hull form parameters as we focus on non-dimensional parameters like F_n and C_B only. Although, the design curves results into desired value for each of the parameters, the interdependencies between the parameters are not considered.

In the process of bulb design, we follow the following orderly steps: 1) Start the design with protruding length L_{PR}, 2) Design the longitudinal section with selected Z_B, 3) Detail the design of the longitudinal section with selected Z_B with satisfying A_{BL}, 4) Detail the design of Step 3 with design of the bulb breadth B_B, 5) Detail the design of Step 4 with design of the transverse section of selected A_{BT}, 6) Design the full three dimensional volume, and 7) Check, modify and revise the sections after checking the $\forall_{BTOT}$ and LCG_B.

Now, depending upon the following:

- Particulars of ship (e.g. B_{MS}, C_B, T, and L_{LWL}),
- To avoid the formation of hard shoulder, and
- To achieve a smooth and faired length of entrance with low angle,

'Steps 1 - 7', result into a bulb design that will normally deviate from the requirements derived from the design figures. Because of the reasons and interdependencies mentioned above normally it is not possible to design the bulb within strict adherence to the parameters derived from Figures. 5 to 7. The proposed design curves are highly meaningful and a closer if not strictly completely adherence to them results into better performance.

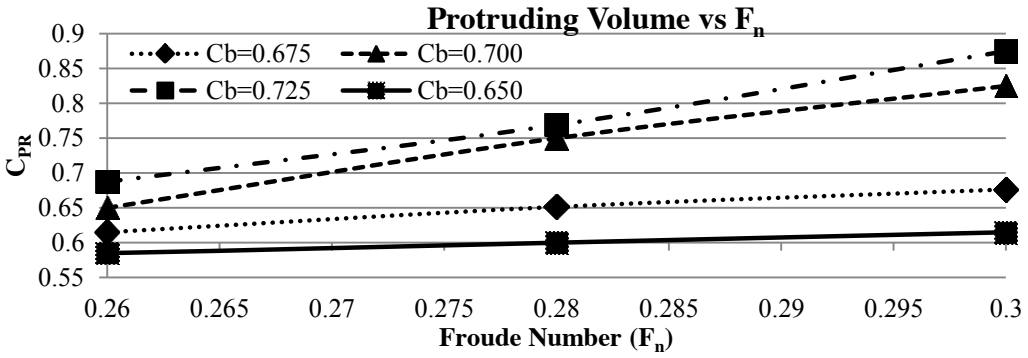

(a) Variation of the protruding volume parameter for a range of the F_n and C_B.

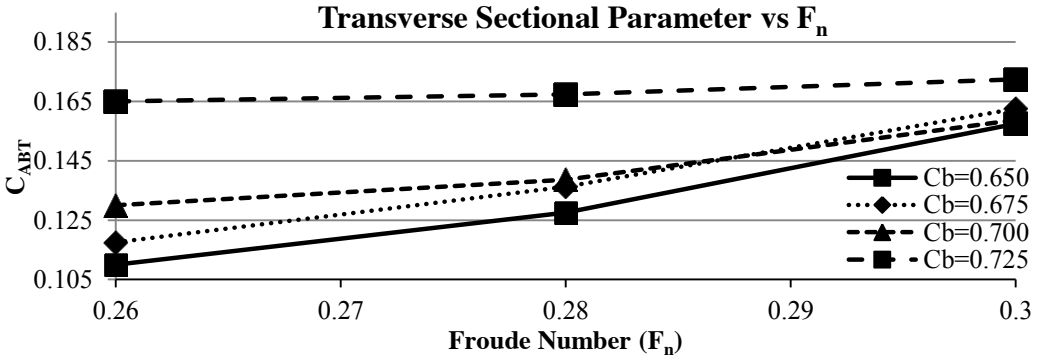

(b) Variation of the transverse cross sectional parameter for a range of the F_n and C_B.

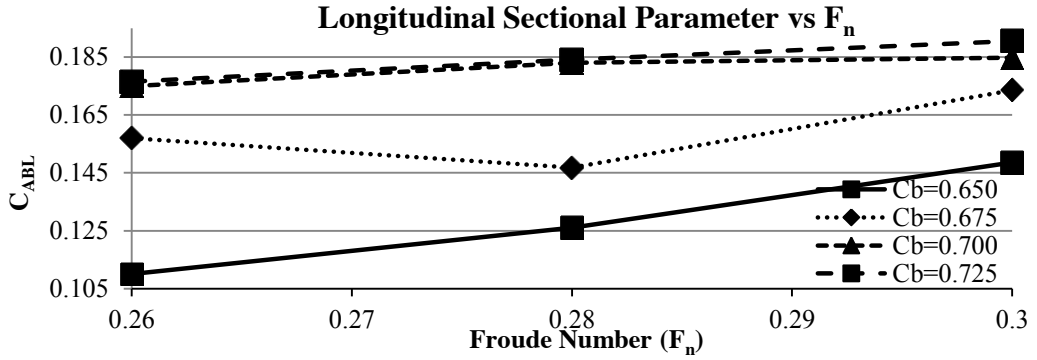

(c) Variation of the longitudinal cross sectional parameter for a range of the F_n and C_B.

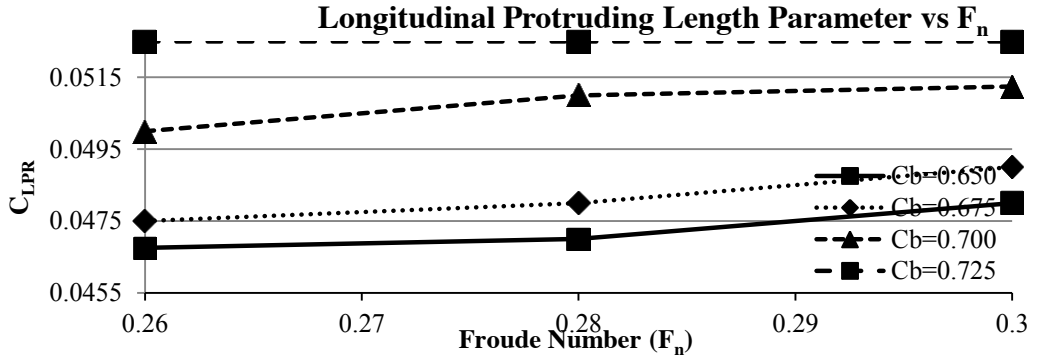

(d) Variation of the longitudinal protruding length parameter for a range of the F_n and C_B.

Figure 5: Variations of the C_{PR}, C_{ABT}, C_{ABL} and C_{LPR} for a range of the F_n and C_B.

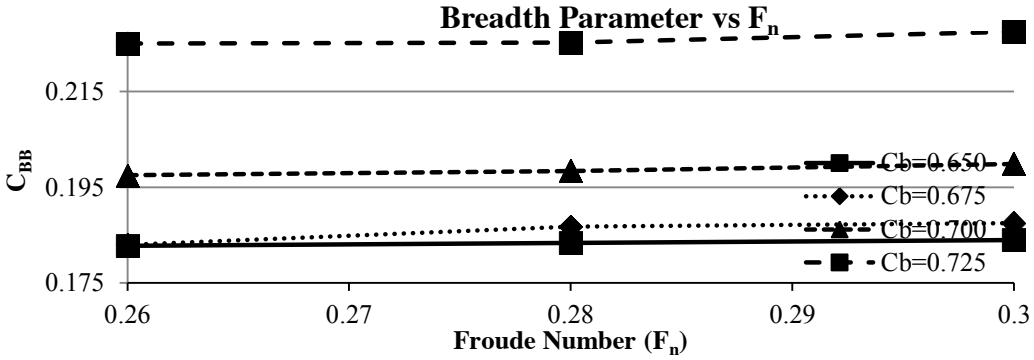

(a) Variation of the breadth parameter for a range of the F_n and C_B.

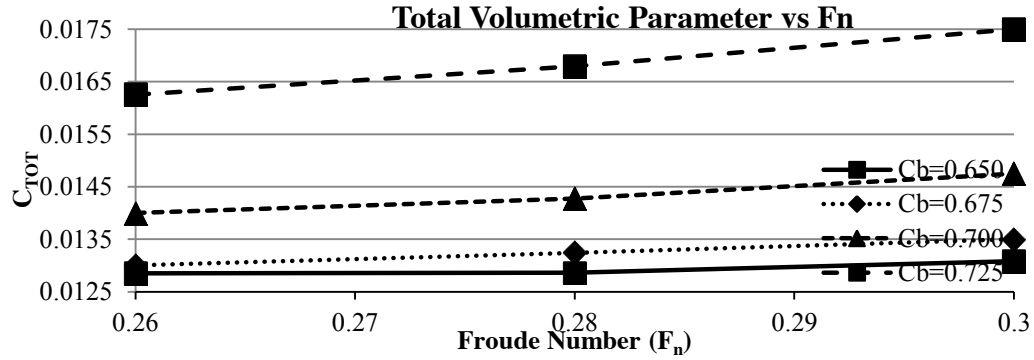

(b) Variation of the total volumetric parameter for a range of the F_n and C_B.

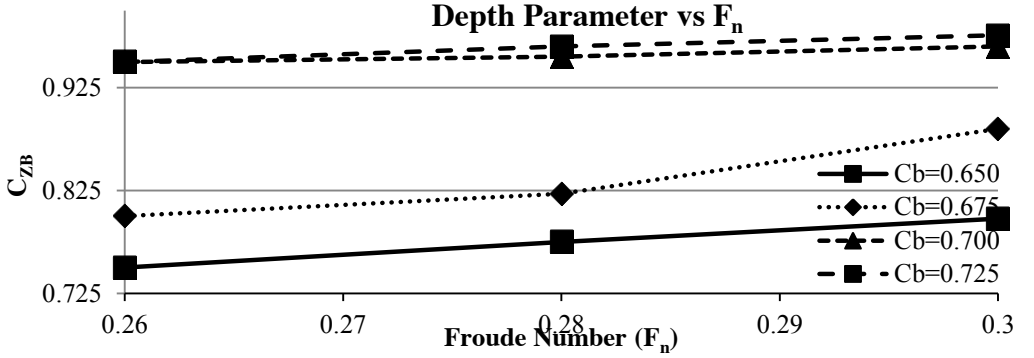

(c) Variation of the depth parameter for a range of the F_n and C_B.

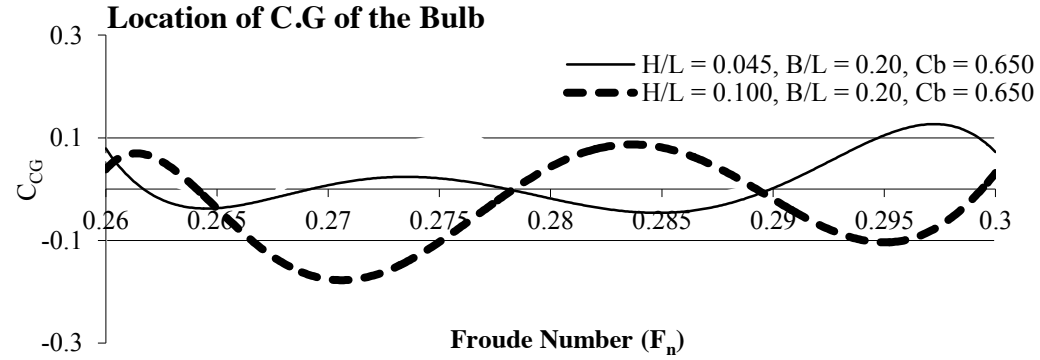

(d) Variation of the location of C.G of the bulb for a range of the H/L, B/L, F_n and C_B = 0.65.

Figure 6: Variations of the C_{BB}, C_{ZB}, C_{TOT} and C_{CG} for a range of the F_n and C_B.

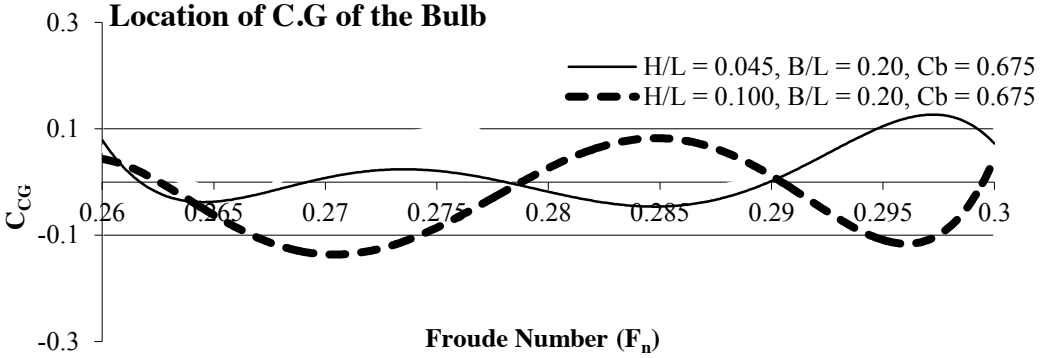

(a) Variation of the location of C.G of the bulb for a range of the H/L, B/L, F_n and C_B = 0.675.

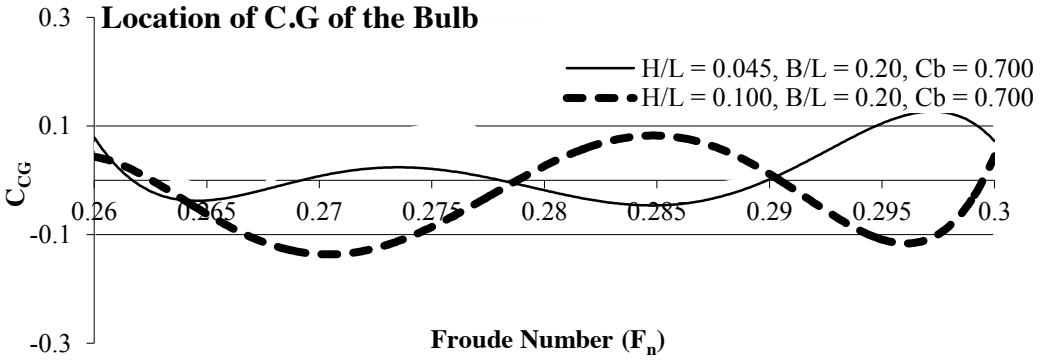

(b) Variation of the location of C.G of the bulb for a range of the H/L, B/L, F_n and C_B = 0.7.

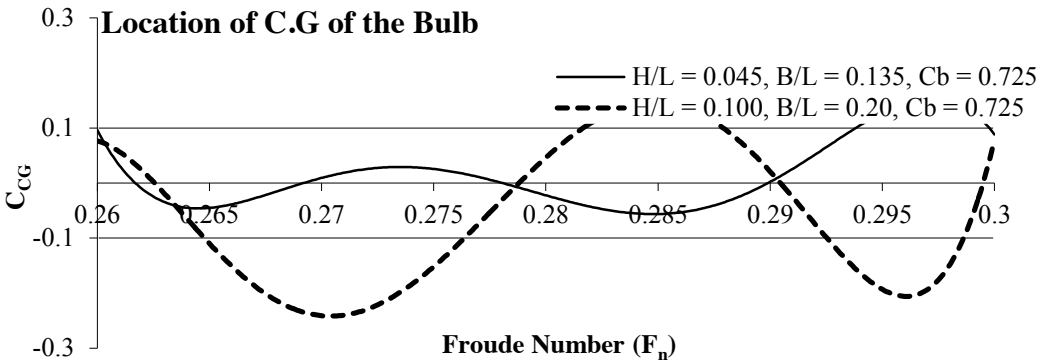

(c) Variation of the location of C.G of the bulb for a range of the H/L, B/L, F_n and C_B = 0.725.

Figure 7: Variations of the C_{CG} for a range of the F_n and C_B across different H/L and B/L.

Additionally, in ship design fairing of lines is subjective and desired preferences for fairing varies from designer to designer. Furthermore, in the area of ship production, the cost parameters are difficult to compute and they are highly subjective to the specific shipyard, e.g. location, size, specialization, and scale of the shipyard, etc.. The shipyard do not share data related to cost and even their preferences, specifications and requirements are not allowed to be reported. Still, from the basic understanding of production, we state that the higher double curvatures, high scantling, larger protruding length of the bulbous bow, and sharper fairing of the bulb to bow, are expected to cost high. In our design process, the opening at the integrated bow has been elongated and the LCG_B (i.e. longitudinal center of buoyancy of the bulb) brought further forward towards of FP. The integrated bulb is of *additive type* rather than *implicit type* and has *nabla shape*. Furthermore, the opening is conical in shape, with sections having a mix of straight and circular shape. In this process of fairing of integrated bulbous bow into the parent container ship, the sections between 16th - 20th stations will alter slightly with an addition of cross-sectional area, and *LCB* will move forward from its original position for the parent container ship. The new design values (in terms of coefficients) of bulbous bow and initial values for KCS's bulb (evaluated at design speed) and the computed dimensions of bulb from of coefficients are listed Table 1. The ID of KCS has a top heavy bulb (*nabla* bulb) and that

is modified under the proposed ship re-design strategy. With the values listed in Table 1, three conventional bulbous bows are used in the present study and these result into three new designs under forward modification. These are analyzed at the design speed using Shipflow[**TM] and after successful modifications of the ship's forward part, an improved design with forward modification is considered for aft modifications further, as described in Section 2.4. The flowchart for re-design strategy is shown in Figure. 8.

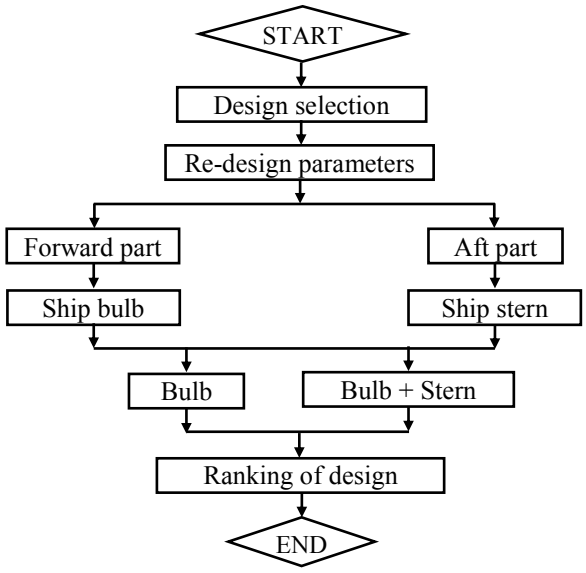

Figure 8: Flowchart of ship re-design strategy.

2.4 SHIP AFT MODIFICATIONS – BASIC IDEA AND GUIDELINES FOR STERN BULB DESIGN

A basic idea to select the frame lines of a stern hull form was suggested by Bessho (1967) and his approach was deduced from the hypothesis of secondary flow energy determined from the potential flow around a double model of hull forms.

As per Bessho (1967), it can be expected that the hull forms having frame lines with a minimum energy of secondary flow show less form drag. Later Asano (1979) explored the further application of the idea of Bessho (1967) to practical cases by showing several numerical examples. Suzuki et al. (2005) extended the works of Bessho (1967) and Asano (1979), and evaluated the energy of secondary flow around double models (without a free-surface effect) by using a potential flow solver. Also, they evaluated the energy of secondary flow by using the Rankine source method to investigate the free-surface effect on secondary flow. And, they suggested optimization methods for stern hull form based on the hypothesis of minimum energy of secondary flow for the cases without and with a free-surface effect. In their optimization process, a 'Non-linear Programming (NLP)' technique was employed to treat design constraints. However, the work of Suzuki *et al*. (2005) is difficult to implement in a fully automatic mode because of the high computational time with successive grid generations and stern form modification process is difficult to define mathematically using the industry standard mathematical definitions (i.e. Non-Uniform Rational B-spline (NURBS), and T-spline, etc.). In the present paper, the basic ideas of Bessho (1967) and Asano (1979), are analyzed along with the results of Suzuki *et al*. (2005) as shown in Figures. 9a, 9b, 9c, and 9d.

Although, an automatic design and fairing of lines is highly desired as it automates the design process and extends itself for close and tighter integration with CFD software, it has limitations because resulting shapes may not be always desirable or producible. In order to avoid this practical inconvenience, a more simplified method is used in this paper.

We note that essentially Bessho (1967) showed that there are ship forms that do not have a secondary flow (e.g. rotational bodies) and on such bodies the stream lines become 'geodesic'. From the differential geometry point of view the geodesic is a generalization of the notion of a 'Straight Line' to 'Curved Spaces'. We explore this concept of geodesic and show it conceptually for implementation in Figure. 9e. We can find the shortest path between two points in a curved space by writing the equation for the length of a curve and then minimizing this length using the calculus of variations. However, this is difficult to implement because here is an infinite dimensional space of different ways to parameterize the shortest path. Hence, it is relatively simple to locally minimizes the length and fair it accordingly. In Figure. 9e, the Cases 1 to 3 show different levels of geodesic and the Case 3 shows the highest level of geodesic and shortest path between the Pt_1 and Pt_3. A further close look at the optimized hull forms of Figure. 9a to 9d and the geodesic description of Figure. 9e reveals that they can be generated iteratively with manual fairing via the processes of 'pulling in' and 'pulling out' of the stations. The processes of 'pulling in' and 'pulling out' of the stations will generate finer and fuller sterns, respectively. Since, the process is manual it is likely to generate shapes that are desirable and producible. However, these processes of 'pulling in' and 'pulling out' of the stations without a proper industry standard mathematical definitions (i.e. Non-Uniform Rational B-spline (NURBS), and T-spline, etc.) cannot be used in automatic generation of stern bulb shape and integrated design environment with CFD. This is a limitation of the work reported in this paper. The ID of KCS has stern tubular bulb (i.e. used for straightening the flow directly at propeller plane for better propulsive efficiency) and that is modified to understand the flow at propeller plane and change in resistance offered by ship in this paper. In aft modifications, ship stern is first made fuller in size and then finer in size using NAPA[*TM] and his is shown in Figure. 10. Starting from the AP three stations (at the station spacing of 11.5 m) are modified to make the stern either full or fine in size.

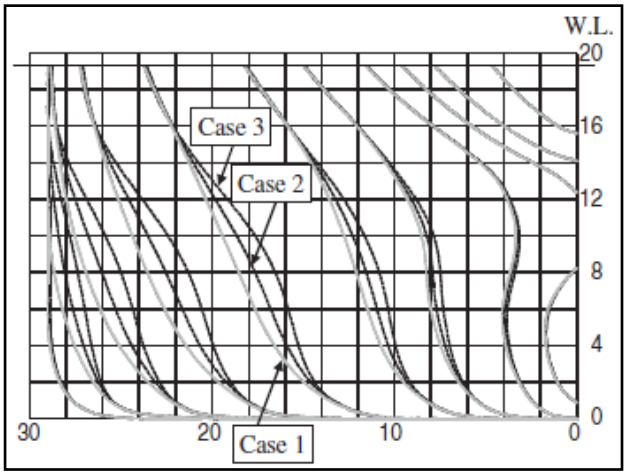

(a) Optimized stern hull forms of SR221B tanker ship.

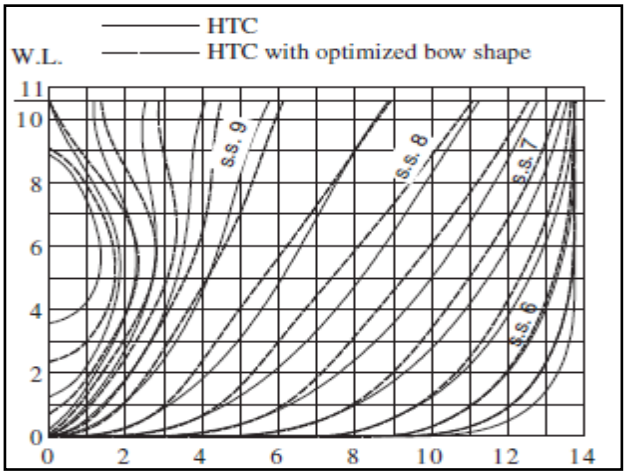

(b) Bow shapes of the initial hull forms in 'Humburg Test Case (HTC)' container ship.

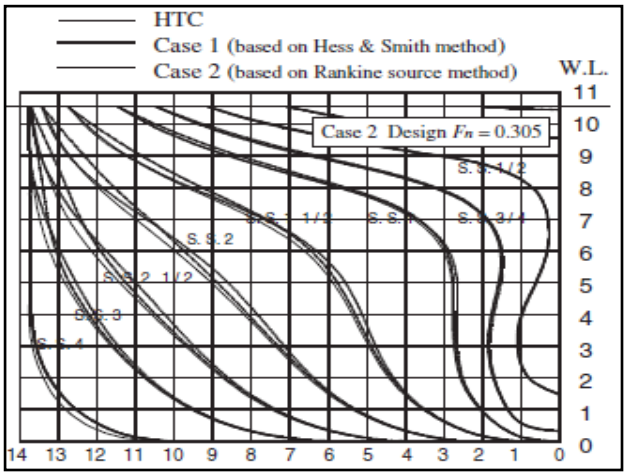

(c) Optimized stern hull forms of HTC container ship.

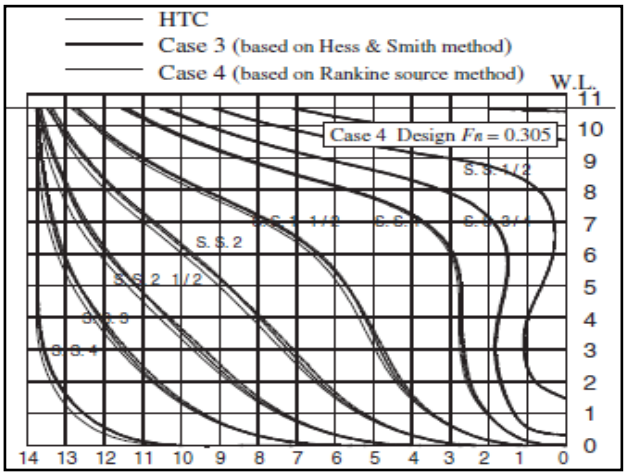

(d) Optimized stern hull forms of the HTC container ship with an optimized bow shape.

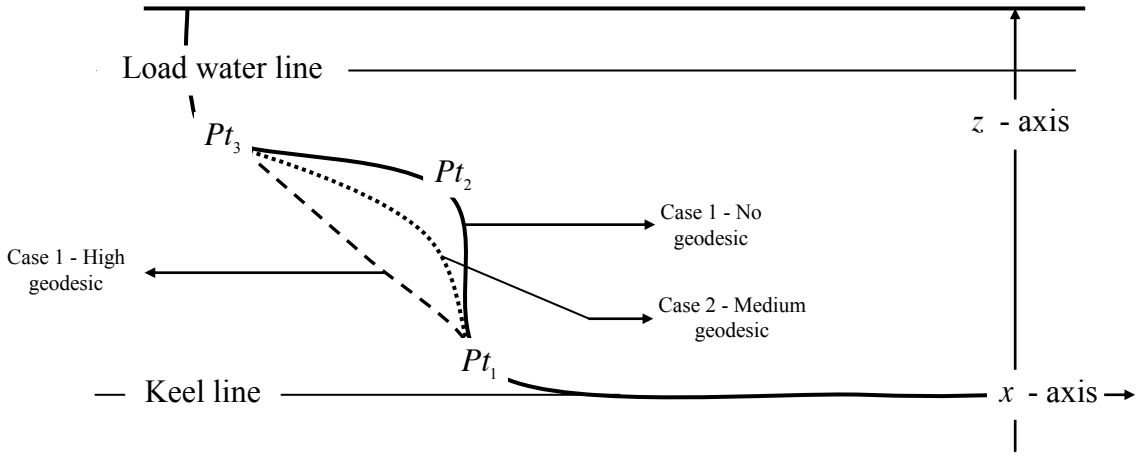

(e) Conceptual description of geodesic for the design of stern frame lines.

Figure 9: Optimized stern hull forms for tanker and container ships and conceptual description of geodesic for the design of stern frame lines, adapted from Suzuki *et al*. (2005)

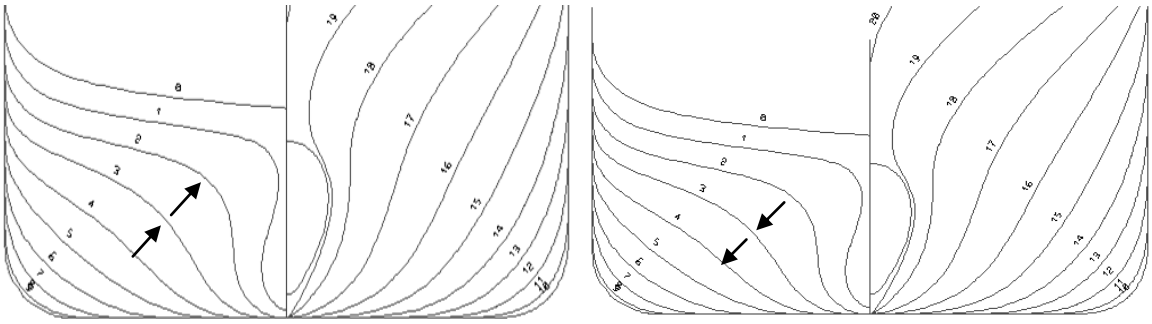

(a) Ship stern made fine in size by 'pulling in' stations. (b) Ship stern made full in size by 'pulling out' stations.

Figure 10: Process of ship stern being made '*finer*' and '*fuller*' in size.

Table 2: Comparison of the LCB and LCF values for new and re-designed ship.

Design types	LCB (m)	LCF (m)
ID - Initial design	111.56	101.91
D1	112.41	102.76
D2	112.00	101.92
D3	111.94	102.00

3. CAD MODEL AND ITS INTEGRATION WITH CFD

3.1 CAD FOR FORWARD MODIFICATION

In this paper, the CAD definition is implemented in NAPA*TM and that has an ease of integration with the handy 'Graphical User Interface (GUI)', CFD software (Shipflow**TM) and other simulation software. The CAD model of KRISO container ship (KCS) is prepared with the offsets available from NMRI (2014) and the profile view has already been shown in Figure3. The forward part of KCS is modified with three types of bulbs bow to study the effect on wave-making resistance. Amongst the three types of bulbs bow, the most efficient one is selected from the CFD analysis and over this most efficient bulb aft part of the ship is modified. All the design alternatives are analyzed for resistance performance and propulsive efficiency. The ID of KCS has a bulbous bow (∇ type) and the new bulbous bow designs are: Design 1 (D1) - Δ type, Design 2 (D2) - O type and Design 3 (D3) - ∇ type.

Ideally, the re-design of bulbous bow includes incorporation of both the linear and non-linear design parameters presented in Figures. 5 to 7 at the same time. However, this is difficult and leads to several design modifications required that will change the ship lines over a larger length in both the fwd and aft of FP. Hence, in order to minimize the changes required in ID of KCS to accommodate the new designs, only the three linear parameters (i.e. B_B, L_{PR}, and Z_B) and two non-linear parameters (i.e. A_{BT} and A_{BL}) are utilized in the re-design. The bulbous bow design parameters are listed in Table 1. Although, the bulbous bow is re-designed to achieve better resistance and propulsive performance of ship, it has effects on the other parameters also, e.g. ship stability, scantling, hydrodynamic motion, and gross revenue, etc. The modifications in the bulb change the position of the 'Longitudinal Center of Buoyancy (LCB)' and 'Longitudinal Center of Flotation (LCF)'. In the present re-design strategy, ship stability is not affected as there are no significant changes in the LCB and LCF values and these are shown in Table 2. It is clear from Table 2 that the changes in LCB and LCF are marginal - less than 0.8%.

The bulb scantling needs to be re-defined because of the complete change in the bulb shape, which is expected to lead to an additional production cost. The additional cost from bulb modification is dependent on the shape of bulb. A bulb with higher double surface curvature costs higher in production. Also, the production cost depends on overall bulb size, bulb scantling, and explicit or implicit nature of bulb, etc. The production cost of explicit bulb is much lower than the implicit bulb because of the extra production cost coming from fairing of bulb near the FP. The ship hydrodynamic motion is not affected much if there are no major modifications in the bulb. Furthermore, some sections aft of the FP are modified to adjust the changes from bulb side. The

increased dimensions of the bulb demand for fairing the forward flow entrance, and these result into major modifications in ship forward stations that are near the bulb (i.e. where the bulb volume is concentrated). As ID of KCS has ∇ type bow, O type and Δ type bow have demanded more modifications in the forward stations. The surface fairing is analyzed from the curvature plots in NAPA*TM. Re-designed bulb shapes and perspective view of bulb shapes are shown in Figures. 11a, 11b, 11c and 11d respectively.

In the present paper, it has been pre-considered that, there is no abominable effect in ship hydrodynamic motion. It is undisputable that bulb re-design will add to overall cost of the ship. However, the re-design leads to better resistance and propulsive performance and that leads to fuel savings resulting into better profit and operating economics of the ship. These savings justify the additional cost that is incurred in production of re-designed ship.

3.2 CAD FOR AFT MODIFICATION

After the forward modifications, further modifications are done in the aft part of the ship. Essentially, two strategies are followed for aft modifications: 1) stern bulb expansion and 2) stern bulb contraction. The stern bulb expansion results into generation of additional volume and contraction results into loss volume for the ship. The stern modification is studied with four different designs each for 1) stern bulb expansion and 2) stern bulb contraction. Each of the stern design alternatives is studied for the forward speed and propeller performance is studied from the wake study using Shipflow**TM. The stern design alternatives are: S1-1D3, S1-2D3, S1-3D3, and S1-4D3 pertaining to stern bulb expansion and S2-1D3, S2-2D3, S2-3D3, and S2-4D3 for stern bulb contraction. And they are generated by modifying the stern bulb. Under the stern bulb modifications, the changes in stern bulb lines at AP have been shown in Figures 12a and 12b. The change in volume for stern design alternatives and their corresponding LCB and LCF values are listed in Table 3 and it is clear that the changes in LCB and LCF are marginal – less than 0.5%. For the sake of completeness, the 'Lines' drawing of ID and all modified designs i.e. forward modifications and aft modifications are reported. Figure. 13a shows the lines drawing of ID. Figures. 13b, 13c, and 14a present the lines drawing of D1, D2 and D3 respectively. The lines drawing of Designs S1-1D3, S1-2D3, S1-3D3 and S1-4D3 (expansion of stern bulb) are shown in Figures. 14b, 14c, 15a and 15b respectively. The lines drawing of Designs S2-1D3, S2-2D3, S2-3D3 and S2-4D3 (contraction of stern bulb) are presented in Figures. 15c, 16a, 16b and 16c respectively.

4. CFD ANALYSIS, BASIC GOVERNING EQUATIONS AND 'VERIFICATION AND VALIDATION (V&V)' STRATEGY

4.1 CFD BASED HYDRODYNAMIC ANALYSIS

The hydrodynamic problem of interest in this paper is mathematically modeled using basic fundamentals of fluid mechanics, ship hydrodynamics and computational fluid dynamics and this mathematical model can be numerically solved with many commercially available CFD software programs, e.g. Shipflow**TM, ANSYS***TM, and STAR-CCM+****TM, etc. However, we use the Shipflow**TM because: 1) it is integrable with NAPA*TM, 2) it has efficient free surface computations, and 3) it has been especially designed for flow computations that involve free surface, e.g. ships. The different modules along with their objectives of Shipflow**TM are listed in Table 4.

4.2 BASIC GOVERNING EQUATIONS

4.2 (a) Potential flow solver: XPAN

Following TM (2014), the major assumptions in the potential flow solver are: inviscid, irrotational, incompressible, and steady flow. Under these assumptions, Navier-Stokes equations are simplified:

$$\frac{1}{2}\nabla U_i^2 = \rho g - \nabla p, \text{ for } (i = 1,2,3) \quad (1)$$

and the continuity equation:

$$div\, U_i = 0, \text{ for } (i = 1,2,3). \quad (2)$$

The velocity vector is written in gradient of a scalar (velocity potential), and Bernoulli's equation and continuity equation are:

$$U_i = \nabla\phi, \quad (3)$$

$$p + \rho g z + \frac{1}{2}(\nabla\phi \cdot \nabla\phi) = \text{Constant}, \quad (4)$$

$$\nabla^2\phi = 0 \quad (5)$$

where ρ is the fluid density, g is the gravitational acceleration, p is the pressure, ϕ is the velocity potential, and U_i $(i = 1,2,3)$ are the components of instant velocity in x, y and z directions respectively. The continuity equation transforms into Laplace equation which is linear and homogeneous which allows superposition of different solutions. The pressure and velocity components are decoupled which makes it possible to solve the Laplace equation first and compute the pressure later.

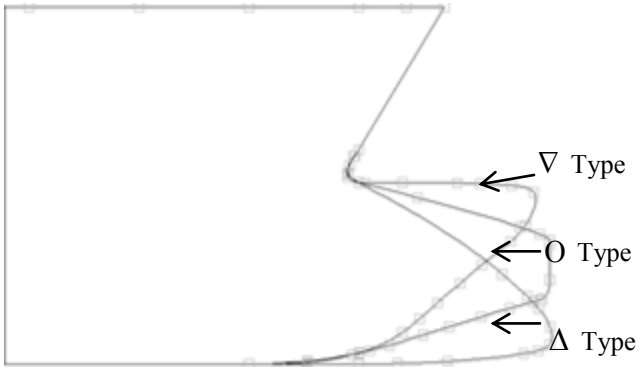

(a) Re-designed bulb shapes.

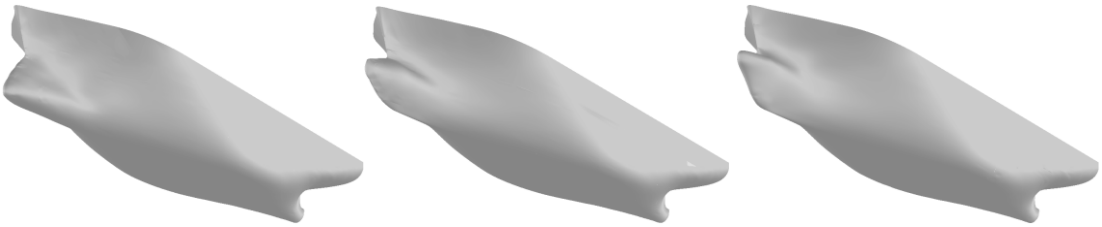

(b) D1 with Δ type bulb. (c) D2 with O type bulb. (d) D3 with ∇ type bulb.

Figure 11: Re-designed bulb shapes and their perspective view of the shapes.

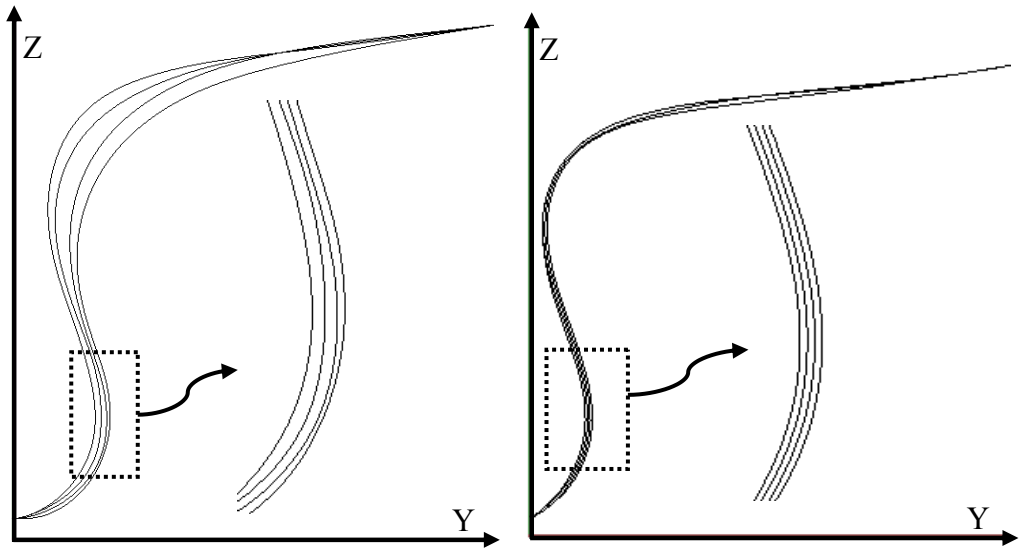

(a) X - section cut at the FP for stern bulb expansion designs.

(b) X-section cut at the FP for stern bulb contraction designs.

Figure 12: Strategies for making stern '*fuller (expansion)*' and stern '*finer (contraction)*'.

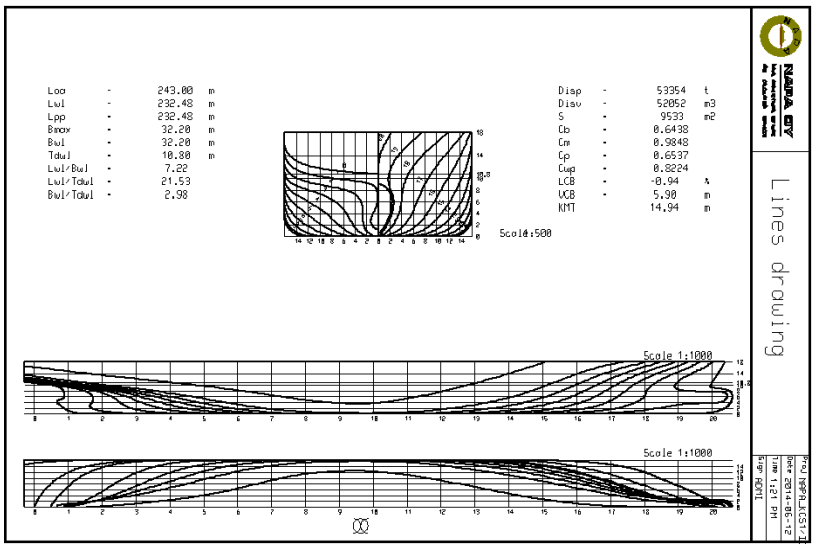

(a) Lines drawing of ID.

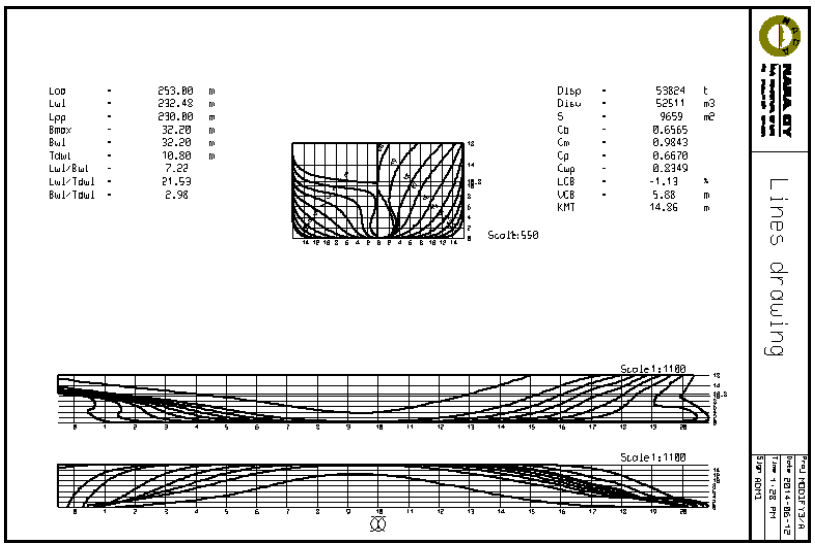

(b) Lines drawing of Design 1.

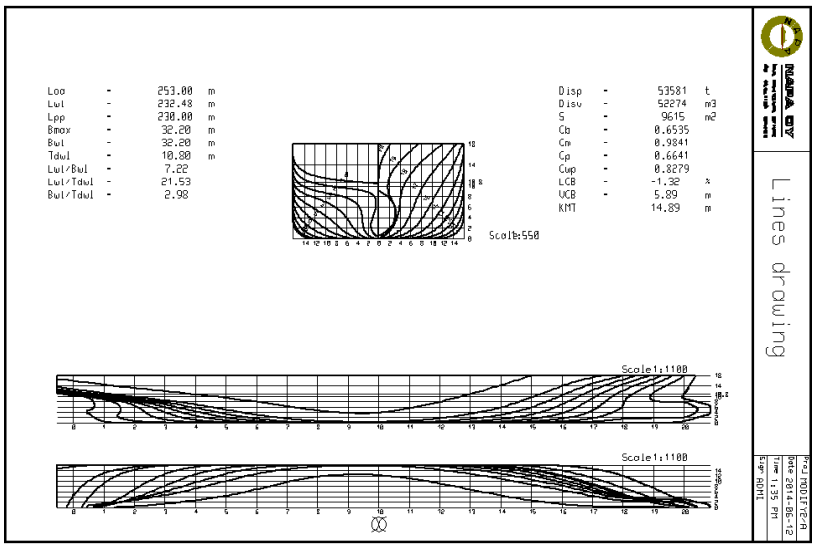

(c) Lines drawing of Design 2.

Figure 13: Lines drawing of ID, D1 and D2.

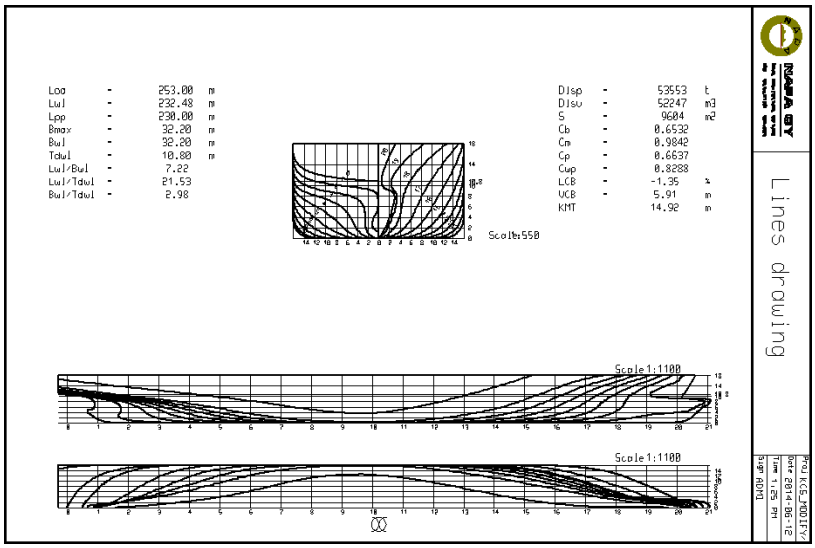

(a) Lines drawing of Design 3.

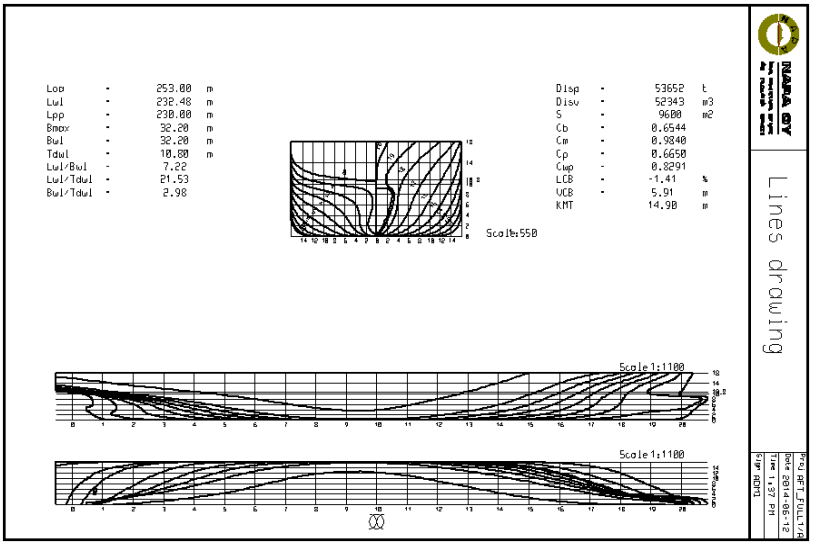

(b) Lines drawing of S1-1D3.

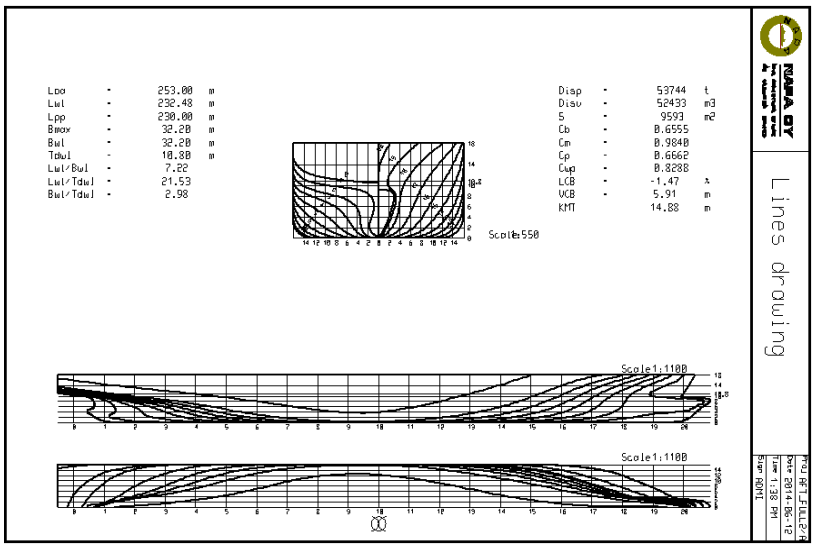

(c) Lines drawing of S1-2D3.

Figure 14: Lines drawing of D3, S1-1D3 and S1-2D3.

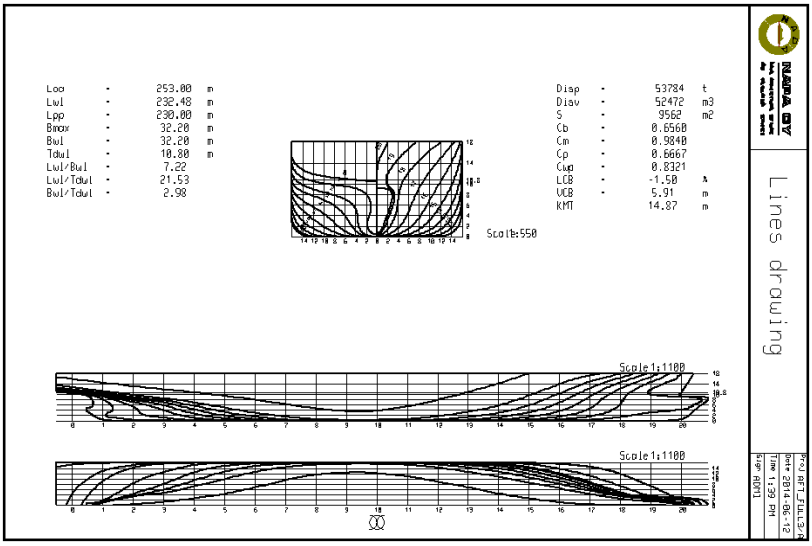

(a) Lines drawing of Design S1-3D3.

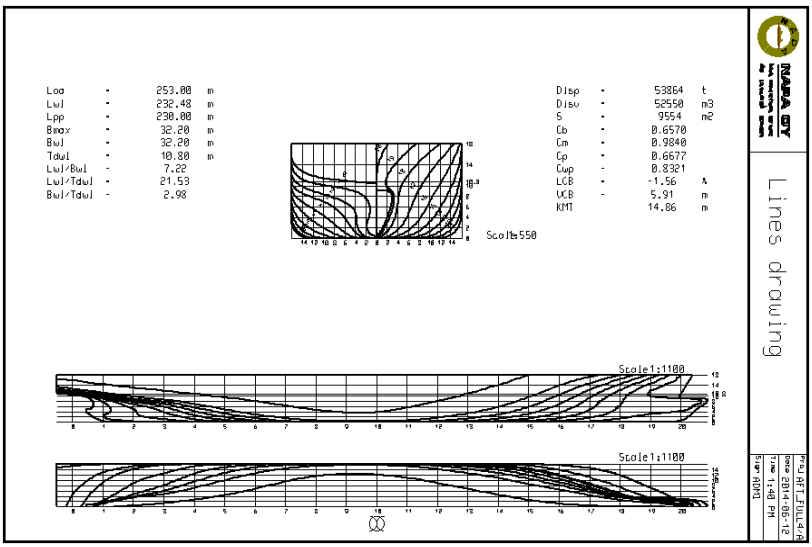

(b) Lines drawing of S1-4D3.

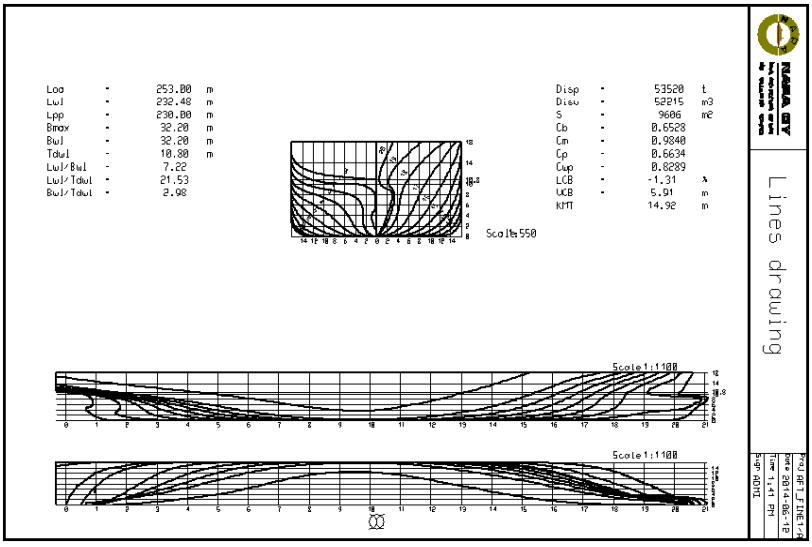

(c) Lines drawing of S2-1D3.

Figure 15: Lines drawing of S1-3D3, S1-4D3 and S2-1D3.

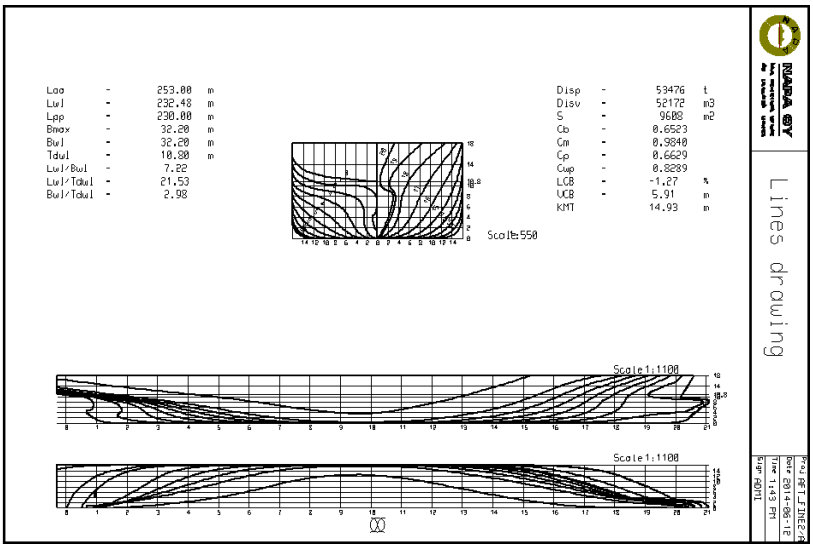

(a) Lines drawing of S2-2D3.

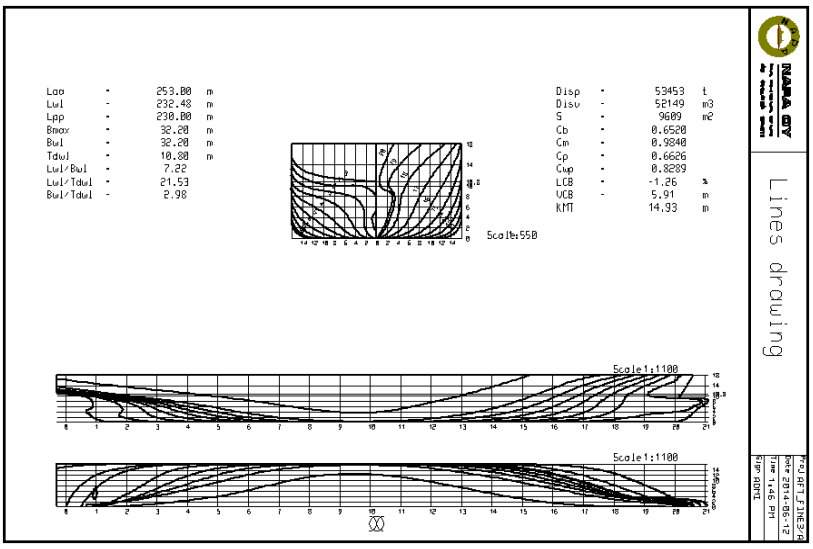

(b) Lines drawing of S2-3D3.

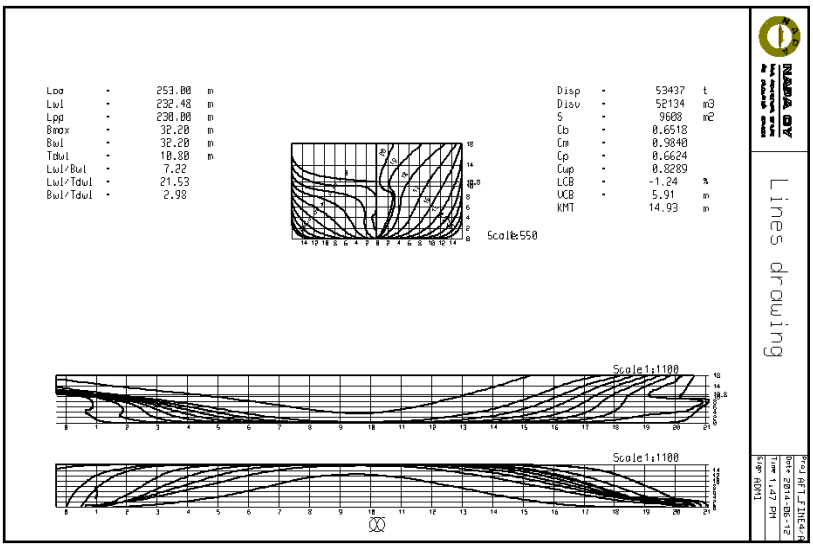

(c) Lines drawing of S2-4D3.

Figure 16: Lines drawing of S2-2D3, S2-3D3 and S2-4D3.

Table 3: Changes in the volume, LCB and LCF values for stern design alternatives.

Stern bulb volume for the fuller shape through expansion			Stern bulb volume for the finer shape through contraction		
Design types	Stern bulb volume (m^3)		Design types	Stern bulb volume (m^3)	
ID	116.43		ID	116.43	
S1-1D3	165.92		S2-1D3	104.00	
S1-2D3	169.36		S2-2D3	100.00	
S1-3D3	230.00		S2-3D3	94.800	
Computed LCB and LCF values for ID and stern expansion designs			Computed LCB and LCF values for ID and stern contraction designs		
Design types	LCB (m)	LCF (m)	Design types	LCB (m)	LCF (m)
ID	111.56	101.91	ID	111.56	101.91
S1-1D3	112.00	101.96	S2-1D3	111.82	101.97
S1-2D3	112.11	101.96	S2-2D3	111.67	101.97
S1-3D3	112.15	102.00	S2-3D3	111.52	101.97
S1-4D3	112.18	102.00	S2-4D3	111.37	101.97

Table 4: Different modules, their objectives and boundary conditions (for XCHAP solver) in the Shipflow[**TM].

Modules and their objectives				
Modules	Objectives			
XMESH	Panel generator for Potential flow module			
XPAN	Flow solver for Potential flow			
XBOUND	Boundary layer computation			
XGRID	Grid generator for viscous computation			
XCHAP	Flow solver for RANS equations			
Boundary conditions for the XCHAP solver				
Parameter	No-slip	Slip	Inflow	Outflow
u	$u_i = 0$	$u_i n_i = 0,\ \frac{\partial u_i}{\partial \xi_B} = 0$	$u_i = \text{constant}$	$\frac{\partial u_i}{\partial \xi_B} = 0$
p	$\frac{\partial p}{\partial \xi_B} = 0$	$\frac{\partial p}{\partial \xi_B} = 0$	$\frac{\partial p}{\partial \xi_B} = 0$	$p = 0$
k	$k = 0$	$\frac{\partial k}{\partial \xi_B} = 0$	$k = \text{constant}$	$\frac{\partial k}{\partial \xi_B} = 0$
ω	$\omega = f(u_\tau, ...)$	$\frac{\partial \omega}{\partial \xi_B} = 0$	$\omega = \text{constant.}$	$\frac{\partial \omega}{\partial \xi_B} = 0$

4.2 (b) Boundary conditions: XPAN

Following TM (2014), the body boundary condition is the tangential flow condition:

$$\phi_n = 0 \tag{6}$$

and there are two boundary conditions for the free surface:

$$\phi_x \eta_x + \phi_y \eta_y - \phi_z = 0 \text{ at } z = \eta(x, y)\,, \tag{7}$$

and

$$P_a + \rho g z + \frac{1}{2}(\nabla\phi \cdot \nabla\phi) = \text{Constant at } z = \eta\,. \tag{8}$$

The solution of Laplace equation for the velocity potential is derived by panel method using Rankine source method on the hull and free surface.

4.2 (c) Viscous flow solver: XCHAP

In Shipflow[**TM], XCHAP is a finite volume code that solves 'Reynolds Averaged Navier-Stokes Equation (RANSE)' and it has the flexibility of using different turbulence models, i.e. 'Explicit Algebraic Stress Model (EASM)', 'Base Line (BSL)' $k-\omega$ model, 'Shear Stress Transport (SST)' $k-\omega$ model. In this paper, the EASM is used because the viscosity term is solved non-linearly in EASM. The governing equations used by XCHAP solver are: 1) momentum conservation, and 2) mass conservation. The momentum conservation equations (Navier-Stokes equations) form RANS equations with time averaging procedures, whereas continuity equation is used as equation of mass conservation. The RANS equations require a turbulence model for closure and

EASM is used for this purpose in the present paper. For an unsteady incompressible flow, the continuity and Navier-Stokes equations can be written:

$$\frac{\partial U_i}{\partial x_i} = 0 \text{ , for } (\text{i} = 1,2,3), \tag{9}$$

$$\rho\frac{\partial U_i}{\partial t} + \rho\frac{\partial (U_j U_i)}{\partial x_j} = \rho R_i + \frac{\partial \sigma_{ij}}{\partial x_j} \text{ , for } (\text{i, j} = 1,2,3) \tag{10}$$

where U_i for $(i = 1,2,3)$ are the components of instant velocity in the x, y and z directions respectively, x_i for $(i = 1,2,3)$ represents the x, y, and z directions respectively, t is the time, R_i for $(i = 1,2,3)$ are the body force intensities in the x, y, and z directions respectively, p is the pressure and μ is the dynamic viscosity of the fluid. The RANS equations are derived from Equation (9) by splitting the instant velocity components U_i, in time mean velocity u_i, and time fluctuating velocity $u_i^{"}$:

$$U_i = \overline{U}_i + u_i^{"} \equiv u_i + u_i^{"}. \tag{11}$$

The σ_{ij} is total stress and for a Newtonian fluid it can be written:

$$\sigma_{ij} = -P\delta_{ij} + 2\mu(S_{ij} - \frac{1}{3}S_{kk}\delta_{ij}), \tag{12}$$

where δ_{ij} is Kronecker delta (i.e. δ_{ij}=1 when i=j, otherwise 0), and $S_{kk} = 0$ for incompressible flow. The S_{ij} is strain-rate:

$$S_{ij} = \frac{1}{2}(\frac{\partial U_i}{\partial x_j} + \frac{\partial U_j}{\partial x_i}). \tag{13}$$

Using Equation (11) in Equations (9) and (10) and carrying out the time averaging procedure, one obtains:

$$\frac{\partial u_i}{\partial x_i} = 0 \text{ , for (} i = 1, 2, 3), \tag{14}$$

and

$$\frac{\partial u_i}{\partial t} + \frac{\partial (u_j u_i + \overline{u_j^{"} u_i^{"}})}{\partial x_j} = \overline{R_i} - \frac{1}{\rho}\frac{\partial p}{\partial x_i} + \frac{\partial}{\partial x_j}(\nu(\frac{\partial u_i}{\partial x_j} + \frac{\partial u_j}{\partial x_i})),$$

where $\nu = \frac{\mu}{\rho}$. (15)

As Reynolds stresses are not known, appropriate turbulence models are introduced for calculating these stresses and their interaction with the mean flow variables and these models are called closure models. Herein, the EASM is used.

4.2 (d) Turbulence Modeling

Following TM (2014), in Boussinesq approximation Reynolds stresses are proportional to the mean strain rate:

$$\rho\overline{u_i^{"} u_j^{"}} = -\mu_T(\frac{\partial u_i}{\partial x_j} + \frac{\partial u_j}{\partial x_i}) + \frac{2}{3}\rho k\delta_{ij} \tag{16}$$

with turbulent viscosity (μ_T) as the constant of proportionality. This concept is based on the assumption that both viscous and Reynolds stresses interact with the mean flow in a similar manner. The main difference between μ and μ_T is that the μ is a property of the fluid whereas μ_T is the property of turbulent flow. On substitution of Equation (16) in Equation (15), the mean flow equation gets additional viscosity μ_T due to turbulence of the flow. One of the many ways to model the turbulence viscosity is the use of linear eddy viscosity approximations and that is used in Boussinesq approximation for the incompressible flows.

4.2 (e) Explicit Algebraic Stress Model (EASM)

Since Boussinesq assumption is a linear model it sometimes fails to give satisfactory results and to improve this, nonlinear terms are added in EASM. The Reynolds stress tensor is then given:

$$\begin{aligned}\rho\overline{u_i^{"} u_j^{"}} = \frac{2}{3}\rho k\delta_{ij} - \mu_T(S_{ij} + a_2 a_4(S_{ik}W_{kj} - W_{ik}S_{kj})) \\ - a_3 a_4(S_{ik}S_{kj} - \frac{1}{3}S_{mn}S_{mn}\delta_{ij})\end{aligned} \tag{17}$$

and the turbulence viscosity:

$$\nu_T = max(-k\alpha_1, \frac{0.0005k}{\beta * \omega}) \tag{18}$$

where α_1 is obtained from:

$$\begin{aligned}&(\frac{\alpha_1}{\tau})^3 - \frac{\gamma_1}{\eta^2\tau^2\gamma_0}(\frac{\alpha_1}{\tau})^2 \\ &+ \frac{{\gamma_1}^2 - 2\eta^2\tau^2\gamma_0 a_1 - \frac{2}{3}\eta^2\tau^2 a_3^2 + 2R^2\eta^2\tau^2 a_2^2}{(2\eta^2\tau^2\gamma_0)^2}(\frac{\alpha_1}{\tau}) = \\ &\qquad - \frac{\gamma_1 a_1}{(2\eta^2\tau^2\gamma_0)^2}\end{aligned} \tag{19}$$

where,

$$W_{ij} = \frac{1}{2}(\frac{\partial U_i}{\partial x_j} - \frac{\partial U_j}{\partial x_i}), \quad \eta^2 = S_{ij}S_{ij}, \quad R^2 = \frac{W_{ij}W_{ij}}{\eta^2},$$

$$a_1 = \frac{1}{2}(\frac{4}{3} - C_2), \; a_2 = \frac{1}{2}(2 - C_4), \; a_3 = \frac{1}{2}(2 - C_3),$$

$$a_4 = \frac{\tau}{\gamma_1 - 2\gamma_0(\alpha_1/\tau)\eta^2\tau^2}, \qquad \gamma_0 = \frac{C_1^1}{2},$$
$$\gamma_1 = \frac{C_1^0}{2} + \frac{C_{\varepsilon 2} - C_{\varepsilon 1}}{C_{\varepsilon 2} - 1}, \; C_{\varepsilon 1} = 1.44, \; C_{\varepsilon 2} = 1.83, \; C_1^0 = 3.4,$$
$$C_1^1 = 1.8, \; C_2 = 0.36, \; C_3 = 1.25, \; C_4 = 0.40. \tag{20}$$

The correct root of Equation (19) is the root with the lowest real part.

4.2 (f) Boundary conditions: XCHAP

The pressure value is being initialized by the values from XPAN results. The inflow is given velocity input and outflow is given as pressure input. The side walls are given as slip conditions and ship surface as the no-slip condition. The inflow boundary conditions are generated from the results provided by XPAN and XBOUND when the zonal approach is used. The different boundary conditions that are used for XCHAP solver are listed in Table 4.

4.2 (g) Computational domain and discretization

The computational domain around KCS is shown in Figures. 17a, 17b and 18a. As container ship is also a displacement vessel which implies that it is fuller in shape in the middle, and finer near stern and bow regions. So, in order to compute the viscous phenomena around the ship hull, a fine mesh needs to be generated near the stern and bow parts of ship. The domain discretizations are: 1) XMESH surface grid for XPAN, and 2) XGRID volumetric grid for XCHAP.

4.2 (h) Surface grid: XMESH

The XMESH is a surface meshing over the ship hull surface and the free-surface that is used for the computation of wave making component of the total resistance. The XPAN is a panel method based solver to solve the potential flow over the panels generated by XMESH. The XMESH can generate both the rectilinear (flat) and curvilinear (parabolic) panels over the body surfaces. The XMESH can be executed as a separate program to check the panels of the body and free-surface before the potential flow computation is executed. The XMESH module is also executed during the potential flow computation when sinkage/trim or non-linear iterations are performed and the panels are updated in each of the iterations. Figure. 19 shows the panels generated over the body surfaces using XMESH command. The XMESH generates two types of panels: 1) flat panels with constant source strength and 2) parabolic panels with linearly varying source strength.

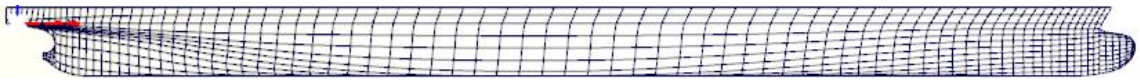

(a) Hull surface grid.

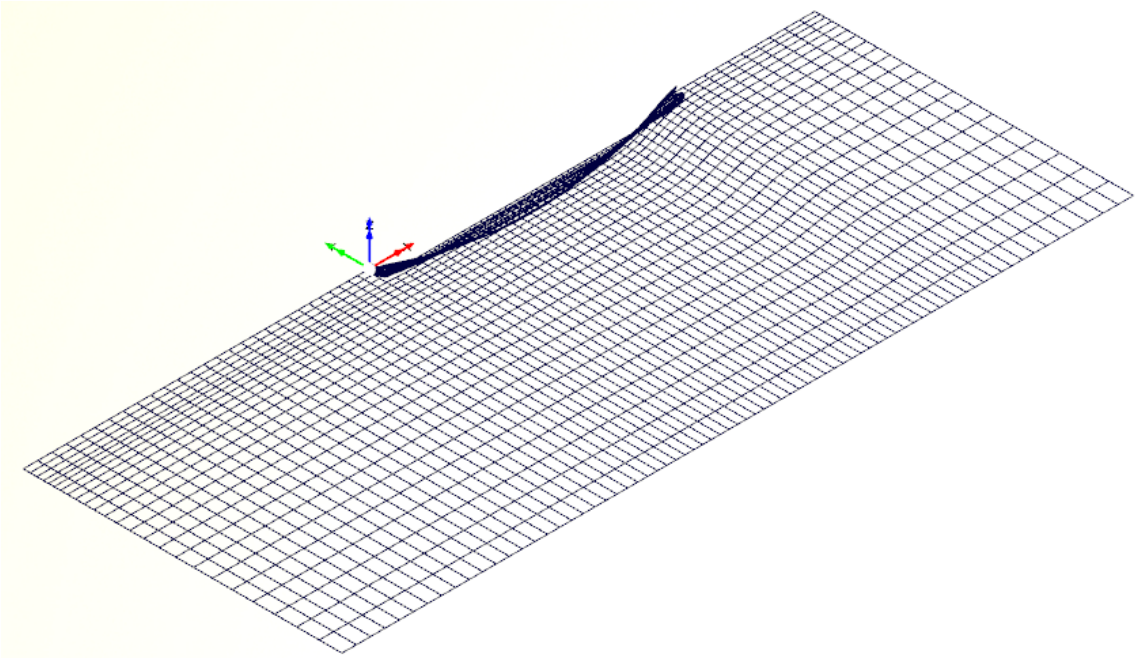

(b) Free-surface grid.

Figure 17: Panel mesh generated by XMESH.

4.2 (i) Volumetric grid: XGRID

The XGRID generates the grid used for the viscous flow computations in XCHAP around a ship and that is used for the computation of the total resistance of ship while running at forward speed. The computational domain for XGRID extends up to $0.5L_{pp}$ upstream of the forward Perpendicular and $1.8L_{pp}$ downstream from the aft perpendicular. A default optimum value for the domain is considered. Also, a grid convergence study is conducted by considering different dimensions of the computational domain. An automated regular structured mesh generated by XGRID is used to study the flow characteristics around the 3-D ship model.

A cylindrical domain is used for the grid generation around the ship and below the still water line as shown in Figure. 18a. A complete analysis of predicting the bare hull resistance of the container ship is conducted only in one medium (water). The presence of air is not considered in this study and which restrict the present study to analyze the breaking of wave at higher speeds. There is a possibility to consider the effect of the air while computing resistance by meshing the domain above the water line also. Though, this facility is provided in XCHAP solver, it has not been explored in the present paper. In Figure. 18s the green, orange, aqua and lime colors represent the no-slip, slip, in-flow, and out-flow boundary conditions respectively. And, a green color represents the surface of the ship. A complete domain is made as one block and the structured grid is generated accordingly. In XGRID, there is no provision to divide complete computational domain in multiple blocks. A structured mesh is generated inside the block and over the ship surface. Interpolation between surface and domain grid is carefully done to avoid leakage which may cause the error in simulation results or diverge the solution.

4.3. VERIFICATION AND VALIDATION (V&V) STRATEGY

In the fluid dynamic simulation, the verification is defined as a process of assessing the numerical uncertainty (U_{SN}) and when the conditions permit estimating the sign and magnitude of simulation numerical error (δ^*_{SN}) itself and the uncertainty in that error estimate (U_{S_CN}). And, the validation is defined as a process of assessing the simulation modeling uncertainty (U_{SM}) by using any benchmark experimental data and, when conditions permit, estimating the sign and magnitude of the modeling error (δ_{SM}) too.

4.3 (a) Integral variable - Total resistance

It is well known in fluid dynamic simulations that CFD simulations are time consuming and the number of iterations determines the time involved in simulation process. The iteration (i.e. one iteration = 10 steps) history of force (F_X) for different grids is shown in Figure. 18b and it is clear that for 200 iterations the convergence is extremely good. In this paper, the simulation is terminated after 200 iterations. However, it can be noticed from Figure. 18b that after 100 iterations the fluctuations in the compuations of force (F_X) for different grids is low and that can also serve a crietria for termination. This will save computational time.

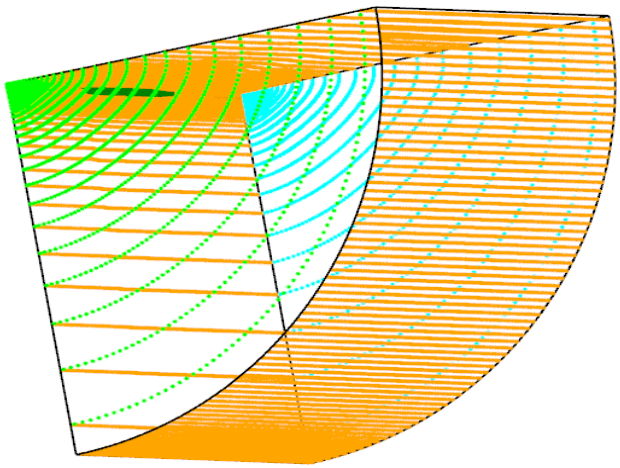

(a) Half of the computational domain for XCHAP.

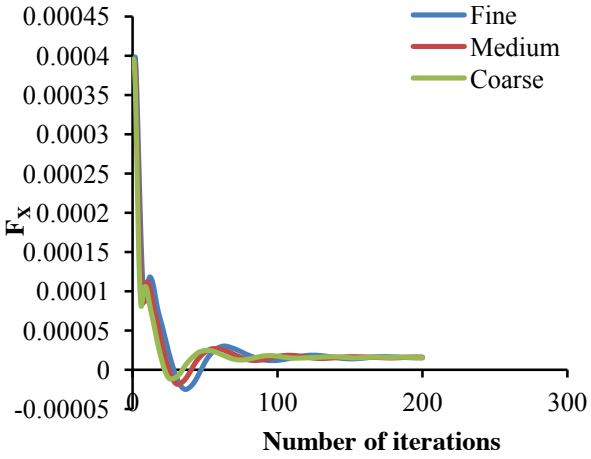

(b) Iteration history of force (F_X) for different grids.

Figure 18: Half of the computational domain for XCHAP and the iteration history of force (F_x) for different grids.

Table 5: Verification of coefficient of total resistance C_T of KCS.

R_G	P_G	C_G	U_G	δ_G^*	U_{GC}	S_C
0.2	4.644	4.000	3.5×10^{-3}	2.0×10^{-3}	1.5×10^{-3}	3.686
		$E\%$	$U_V\%$	$U_D\%$	$U_{SN}\%$	
$E=D-S$		–0.600	0.647	0.640	0.100	

The verification of the total resistance is performed according to the ITTC recommended procedures, ITTC (2008). From the upcoming Section 5, and reference to Table 5, the grid convergence study for C_T is complete and for the unsteady flow computations, the computed total resistance is oscillatory. Therefore, we consider the uncertainty and the convergence ratio R_G is defined:

$$R_G = \varepsilon_{21}/\varepsilon_{32} \tag{21}$$

where $\varepsilon_{k21} = S_{k2} - S_{k1}$ and $\varepsilon_{k32} = S_{k3} - S_{k2}$ give the change of solutions between the medium-fine and coarse-medium grids. Three convergence conditions are possible and they are:

- convergence condition: $0 < R_G < 1$,
- oscillatory condition: $R_G < 0$, and
- divergence condition: $R_G > 1$.

From Table 5, we obtain $R_G = 0.2$ and according to the ITTC (2008), Richardson extrapolation can be used to compute the error for the fine grid and that is:

$$\delta_{RE_G}^* = \varepsilon_{21}/(r_G^{P_G} - 1) = 5.0\times10^{-4} \tag{22}$$

where P_G is the estimated order of accuracy which can be computed as:

$$P_G = \frac{\ln(\varepsilon_{32}/\varepsilon_{21})}{\ln r_G} = 4.644\,. \tag{23}$$

In Equation (23), $r_G = \sqrt{2}$ is considered as a good grid refinement ratio. Furthermore, a correction factor (C_G) is used for estimating the error and the uncertainty of the finest grid solution. This is defined as:

$$C_G = \frac{r_G^{P_G} - 1}{r_G^{P_{Gest}} - 1} = 4 \tag{24}$$

where $P_{Gest} = P_{th} = 2$. For the C_G considered as sufficiently less than or great than 1 and lacking of confidence, the uncertainty is estimated as:

$$U_G = \left|(1-C_G)\delta_{RE_G}^*\right| + \left|C_G\delta_{RE_G}^*\right| = 3.5\times10^{-3}. \tag{25}$$

For the C_G considered as close to 1 and having confidence, both δ_G^* and U_{GC} are estimated as:

$$\delta_G^* = C_G\delta_{RE_G}^* = 2.0\times10^{-3}\,, \tag{26}$$

and $$U_{GC} = \left|(1-C_G)\delta_{RE_G}^*\right| = 1.5\times10^{-3}\,. \tag{27}$$

The corrected solution is defined as:

$$S_C = S_G - \delta_G^* = 3.686\,. \tag{28}$$

The verification results are summarized in Table 5 where $R_G < 0$ gives the monotonic convergence of the solution as per the selected grid types. In Table 5, $U_{SN} = \sqrt{U_G^2 + U_I^2}$ is the simulation uncertainty and $U_V = \sqrt{U_{SN}^2 + U_D^2}$ is the validation uncertainty. It is the standard practice in simulation based design approaches to ensure that within the signatory convention the comparison error (E) is smaller than the validation uncertainty (U_V). Herein too, this criteria is utilized to validate the solution at the U_V interval, for details see Campana *et al*. (2006), Tahara *et al*. (2008), Kim and Yang (2010), Park *et al*. (2015), Huang and Yang (2016). Since, in our analysis the E is smaller than the U_V, the simulation result of C_T is validated. Also, initially a grid independence study is done to nullify any uncertainty present in the selected software module. Furthermore, the performances of different bulb designs are analyzed through the resistance computations, analysis of local flow behavior around bulb, and nominal wake analysis. Hence, we state that our results are validated, verified and reliable.

5. NUMERICAL EXAMPLE AND DISCUSSION

As has been mentioned before, the KCS is used and the modification is divided into two major parts: 1) Forward modification and 2) Aft modification with forward part already modified.

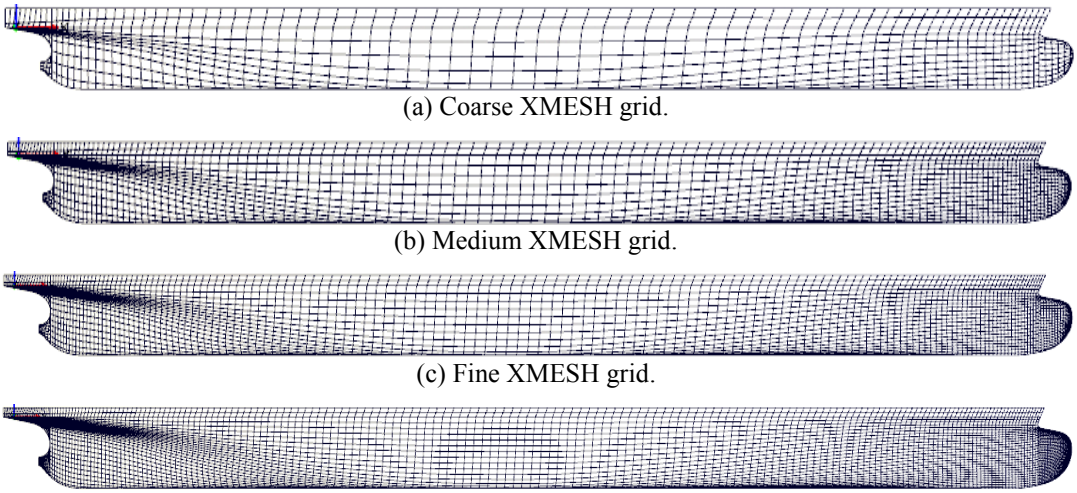

(a) Coarse XMESH grid.

(b) Medium XMESH grid.

(c) Fine XMESH grid.

(d) Very fine XMESH grid.

Figure 19: Different XMESH grids over the hull surface.

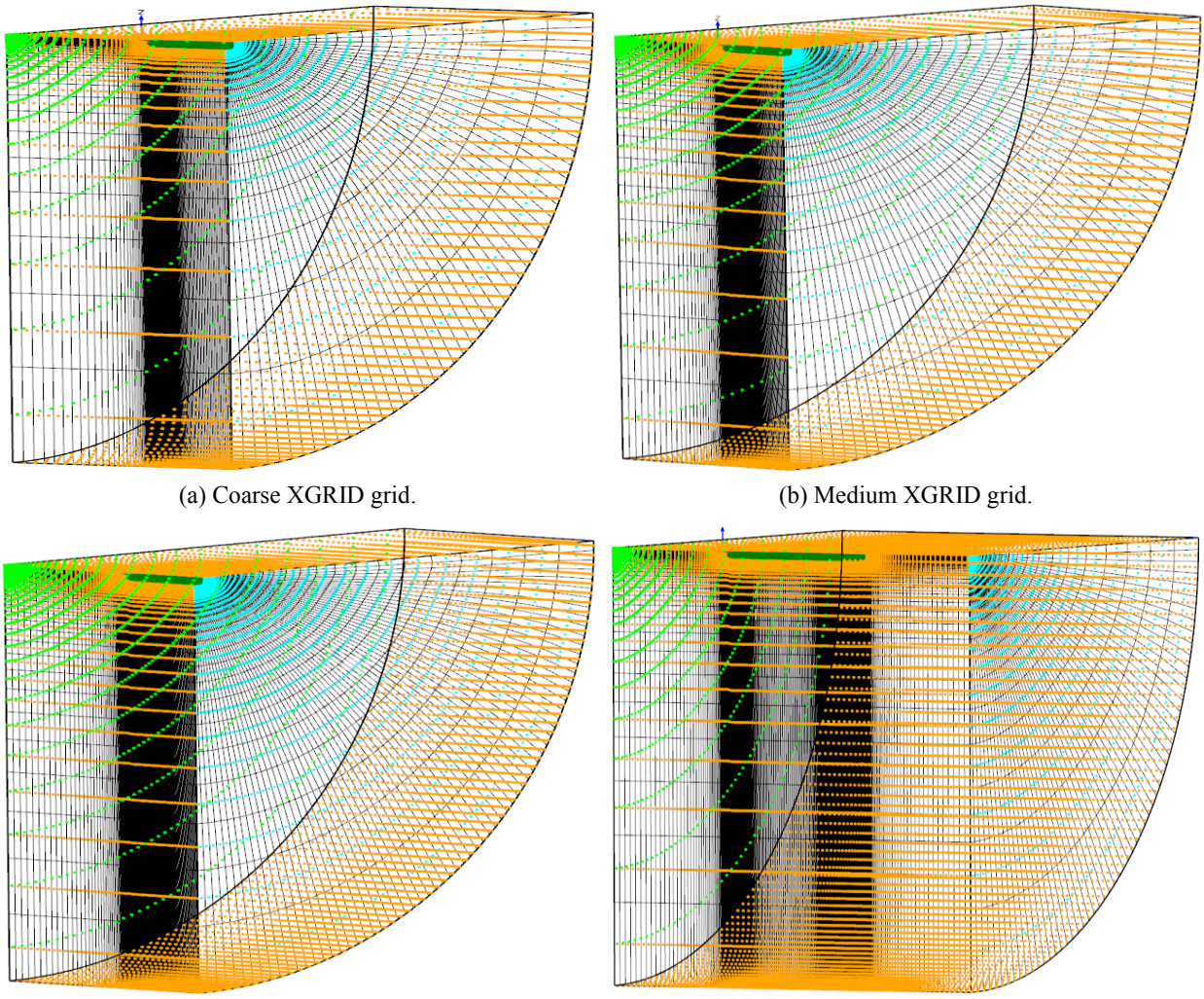

(a) Coarse XGRID grid.

(b) Medium XGRID grid.

(c) Fine XGRID grid.

(d) Global approach XGRID grid.

Figure 20: Different XGRID over a computational domain.

5.1 GRID CONVERGENCE STUDY

We focus on two solvers: XPAN and XCHAP. The XPAN is a potential flow solver and XCHAP is a turbulent flow solver and they are used for the prediction of C_W and C_T, respectively. The surface grid (panels) used for the XPAN solver is shown in Figure. 19. The volume grid used for the XCHAP solver is shown in Figure 20. Table 6 shows the grid convergence study of the XPAN and XCHAP solvers at the V_S = 24 knots. We note here that the grid convergence study is conducted for the scaled model of KCS design. For the XCHAP a volume grid with 1.2 million elements (fine XGRID) is considered over a grid of 0.7 million elements (medium XGRID) for the further CFD study irrespective of the time taken for the complete analysis. Because, as ship is undergoing design modifications, fine XGRID is considered to be the better option to closely capture the flow characteristics. A longitudinal wave cut is plotted in Figure. 21a for all types of the XMESH grid to analyze the effect of increased number of panels over a hull surface.

5.2 VALIDATION OF NUMERICAL RESULTS AT FORWARD SPEED

The laboratory experiments available from NMRI (2014) are used for the validation in present paper. The validation is done for the model ship KCS (geometric scale: 1:31.6). Table 7 shows comparison of the C_T and C_W with the laboratory results and computed results. Figure. 21b shows the comparison of the longitudinal wave cut with the laboratory results and computed results. All the results are computed and compared at constant draught ($T = 0.342$ m). The results show good agreement with very low percentage of error (i.e. within +/- 3.75 %) and within the signatory convention the E remains smaller than the U_V (i.e. within +/- 4.25 %).

5.3 FORWARD MODIFICATIONS

In this paper, the bulbous bow is re-designed by extending an earlier method (Sharma and Sha (2005b)) which gives new design parameters for the existing bulb. Also, other two conventional shapes of bulb profile (i.e. Δ type and O type) have been experimented to study the alternate design for better ship hull performance.

It is clear from Figure. 6c that the desired bulb section of KCS re-design/modification is of ∇ type. However, we explore the other two types (i.e. O and Δ types) also because of the following reasons:

- A bottom heavy bulb (Δ type): It suits the oil tanker ships because even at the lower draft (i.e. ballast draft) the bulb remains submerged, fully wetted and ensures less chances of coming out of water in slamming condition. However, the bulbous bow design will be for the fully loaded condition because the gains will be higher at the higher displacement. So, from the design point of view, only the C_{ZB} will not follow the design charts related to the fully loaded condition (i.e. higher block coefficient C_B, displacement $\forall_{WL}$ and speed V_S). On the other hand a top heavy bulb in the lower draft (i.e. ballast draft) will not remain submerged, not be fully wetted and have higher chances of coming out of water in slamming condition.

Table 6: Grid convergence studies of the XPAN and XCHAP solvers.

Convergence study of the XPAN solver.			
XMESH grid type	Number of elements	Wave making resistance co-efficient (C_W)	Difference (in %)
Coarse	2692	4.964×10^{-4}	NA
Medium	6699	6.298×10^{-4}	26.87
Fine	10622	6.7796×10^{-4}	7.647
Very fine	17612	6.7792×10^{-4}	- 0.006
Convergence study of the XCHAP solver.			
XMESH grid type	Number of elements	Total resistance co-efficient (C_T)	Difference (in %)
Coarse	446368	3.6910×10^{-3}	-
Medium	744372	3.6900×10^{-3}	- 0.0270
Fine	1218078	3.5814×10^{-3}	- 2.9430
Global approach	1742262	3.5817×10^{-3}	-0.0084

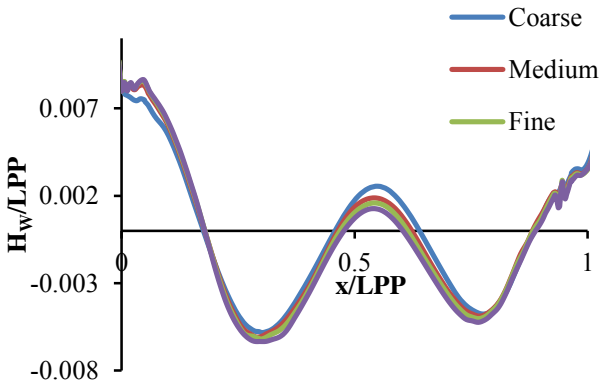

(a) Longitudinal wave cut for the model scale KCS design.

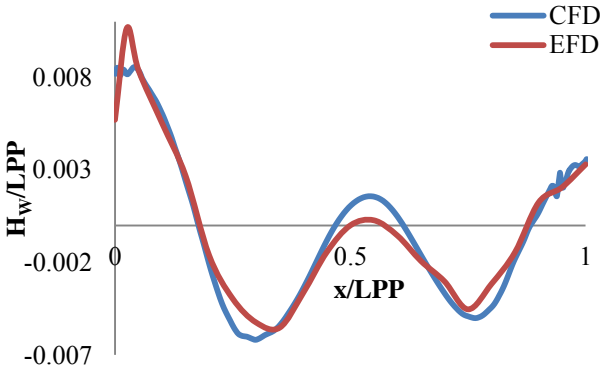

(b) Validation of the longitudinal wave cut at $y / L_{pp} = 0.07$ for the model scale KCS design.

Figure 21: Longitudinal wave cut and its validation at $y / L_{pp} = 0.07$ for the KCS scaled model.

Table 7: Forward speed validation of the CFD results with experimental results.

Parameter	CFD	EFD	Difference (in %)
Coefficient of total resistance (C_T)	3.5814×10^{-3}	3.56×10^{-3}	0.60
Coefficient of wave-making resistance (C_W)	6.7796×10^{-4}	6.88×10^{-4}	- 1.46

Table 8: Design types and the corresponding C_T, nominal wake and volume gain values.

Design name	Bulb type	C_T	Difference (in %)	Nominal wake (w_n)	Volume gain (m^3)
Initial Design	∇ (nabla) type	2.2800×10^{-3}	-	0.195	–
Design 1	Δ type	2.2284×10^{-3}	2.513	0.194	194.0
Design 2	O type	2.2220×10^{-3}	- 2.544	0.196	221.0
Design 3	∇ (nabla) type	2.2010×10^{-3}	- 3.500	0.194	453.7

- A symmetrical sectional bulb (O type): It is production friendly because at least in some parts single curvature shapes can be adopted. This application of single curvatures reduces the manufacturing cost. Furthermore, a symmetrical section means that the L_{LWL} does not change much even when there is significant changes in the loading drafts. This is desired because depending upon the loading weights almost all the ships (i.e. container, cargo and oil tanker ships) show draft variations.

Hence, for the sake of complete and through investigations we focus on all three types of the bulb sections. Different design types for forward modifications are listed in Table 8 and their corresponding C_T values. From Table 8, Design 3 shows an improved value of the C_T at design speed. However, it is well known that gain in resistance may be lost at the propulsive side. Hence, in order to check the propulsive performance of new designs wake study is conducted at the design speed and it is also reported in Table 8. Also, the volume gain in each of design modifications is listed in Table 8. As Design 3 shows over all better performance it is studied further for the different F_n and the results are shown in Figures. 22a and 22b. And, it can be clearly observed that Design 3 shows consistent improvement in the performance even with the increasing F_n.

5.4 ANALYSIS OF THE LOCAL FLOW BEHAVIOR AROUND BULBOUS BOW

A flow around ship hull is mainly influenced by ship bow profile and opening of the flow that is created by the bulbous bow. A smooth and faired opening with low angle of entrance creates a streamlined entry of the flow. We aim for a flow opening with these features and in the present re-design strategy, three bulb types are adopted as mentioned in Section 5.3.

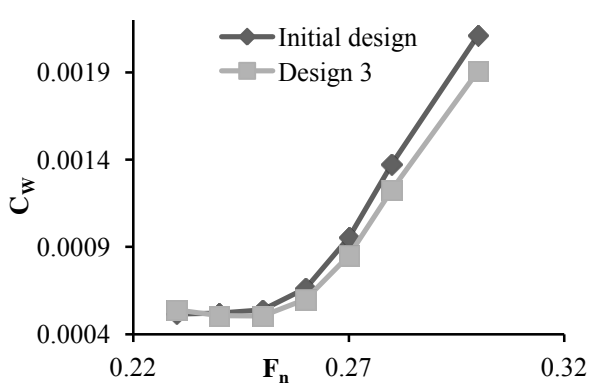

(a) Comparison of C_W values at different F_n for the ID and Design 3.

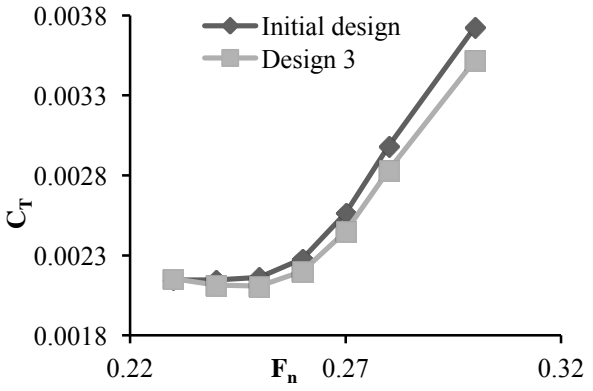

(b) Comparison of C_T values at different F_n for the ID and Design 3.

Figure 22: Comparison of C_W and C_T values at different F_n for the ID and Design 3.

5.4 (a) D1 – Δ type bulb

The Δ type bulb has more concentrated volume towards the keel line which creates an easy opening in the vertical direction whereas it gets narrower near the keel line. As a result of that, more and water rush vertically and remaining water gets accelerated following the keel line. This results into a larger coverage of the bulb with flow of higher vertical velocity (in z direction), refer to Figure. 23. As the flow tries to follow the keel line and the sharp gradient exists in 'D1', the flow gets accelerated and tends to separate early. This results into an increase in the ship resistance.

5.4 (b) D2 – O type

The O type bulb is symmetric about the x-z plane and it a compromise design between the two extreme shape profiles, e.g. Δ and ∇ types. The symmetric part of bulb enables the flow to be equally distributed in a balanced manner above and below the axis of symmetry (x-axis). This type of bulb results into a circular/elliptical/spherical opening depending upon the bulb sections and their fairing into the sectional area curve. A symmetric section is known to generate a scattered flow or a flow with splash effects. A scattered flow with proper gradient changes ensures that the vertical component of velocity changes smoothly and has lower values. Furthermore, the distribution of vertical component of velocity around the O type bulb is more uniform as compared to the Δ type bulb and that is visible in Figure. 23. This results into marginal improvement in the resistance as listed in Table 8.

5.4 (c) D3 – ∇ type

The ∇ type bulb has more concentrated volume towards the water line and it reduces towards the keel line. This arrangement results into a parabolic opening with sharp gradient towards the bow keel. The flow starts and then with gravity accelerates towards the bow keel and as the bow keel profile is made sharp, the flow remains close and attached to the ship hull and does not separate at a shorter length. This not only ensures that the vertical velocity is low (from Figure. 23) it also ensures that the majority of the bulb area is covered with average vertical velocity. This results into a favorable resistance performance. As shown in Table 8, D3 shows significant improvement in the total resistance compared to ID and other forward modification design alternatives.

In D3 the wave-making resistance is reduced by around 9.65% as compared to ID which is advantageous when operating the ship at higher speed. The ∇ type bulb has fair flow opening compared to Δ and O types and that enables the flow to following the bow keel and change only gradually. This gradual change in C_P is shown in Figure. 24a and 24b and in comparison to the initial design it is even more clear. Figures. 24c and 24d show the resultant velocity vector plot and the velocity vectors closely follow the bulb profile with more straight velocity vectors in D3 than ID near the top side of bulb and they contribute in low bow generated wave height.

An improvement in the resistance may not result into the improvement in delivered power also. In this regard, we compute the nominal wake for both ID and Design 3 and that is shown in Figure. 25a and 25b. And it is almost identical with which does not affect the propulsive performance under the design modifications.

In order to analyze the local flow behavior around bulbous bow, the pressure distribution around the ship bow is studied. The Figure. 24 shows comparison between ID (initial design of KCS ship) and D3. It is indicative that D3 shows gradual change in the pressure at the forward part of ship as compared to the initial design. The velocity vector plot around the bulbous bow

is shown in Figures. 24c and 24d. The flow over bulbous bow in case of ID is similar to flow over a sphere. And because of this, water is forced to go down the bulbous bow which results in to the gradual increase of bow height. In D3 the flow opening gets smooth and that results into reduced wave height as compared to the ID. Furthermore, the distribution of velocity and pressure around bulbous bow in the ID is relatively poor and that too can result into elevated wave pattern near the bulb. The increase of bow height results into additional resistance as is predicted using CFD. Similarly, D1 and D2 also show poor resistance as compared to D3. This has been shown in Table 8. Additionally, the flow characteristics near the stern are analyzed and Figure. 23 shows the contour plot of a vertical component of the resultant velocity (V_Z) near stern for all the three modified designs. From Figure. 23, the velocity gradient appears to be smooth in the case of D3 as compared to D2 and D1. Also, the average values of vertical component of the velocity are much lower in the case of D3. The gain in volume for each of alternate designs from the forward modifications is listed in Table 8. The computed nominal wake contours for ID and D3 are shown in Figures. 25a and 25b and they are almost identical. It shows that there is no propulsive performance loss expected in D3.

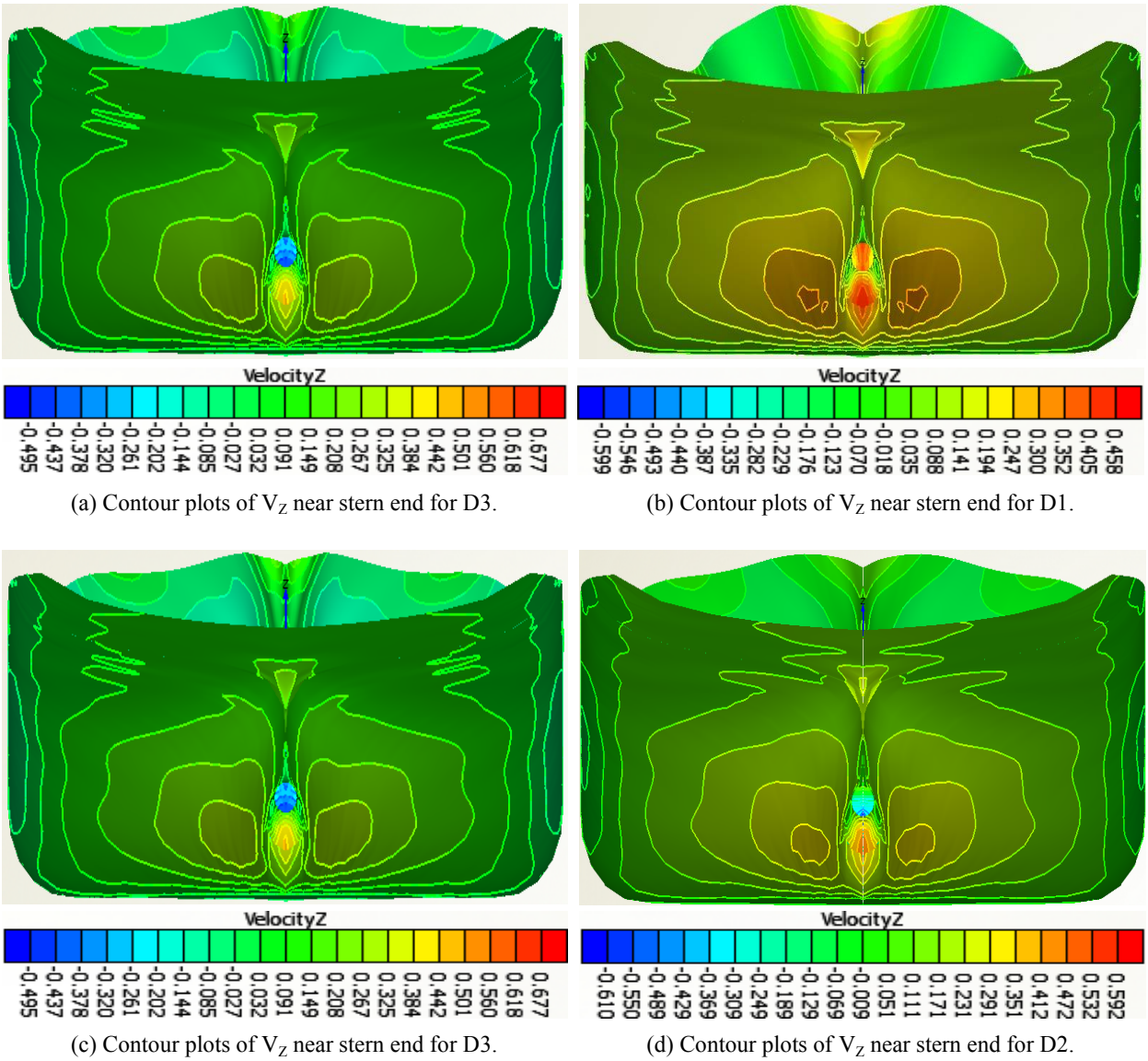

(a) Contour plots of V_Z near stern end for D3.

(b) Contour plots of V_Z near stern end for D1.

(c) Contour plots of V_Z near stern end for D3.

(d) Contour plots of V_Z near stern end for D2.

Figure 23: Contour plots of V_z near stern end for D1 and D3, and D2 and D3.

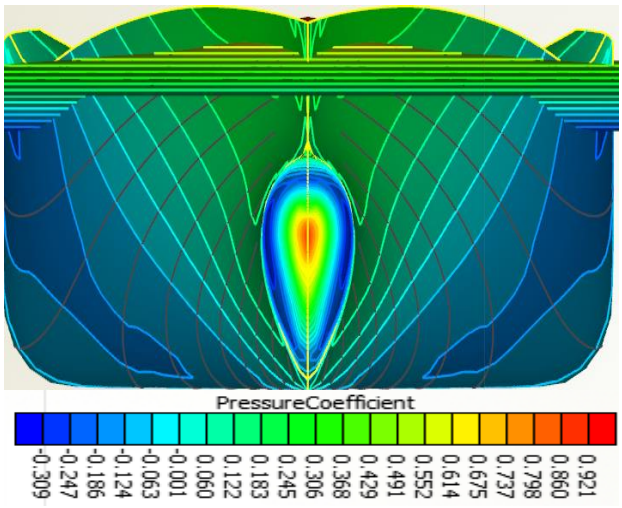

(a) Contour plot of C_P around the bulbous bow for the ID.

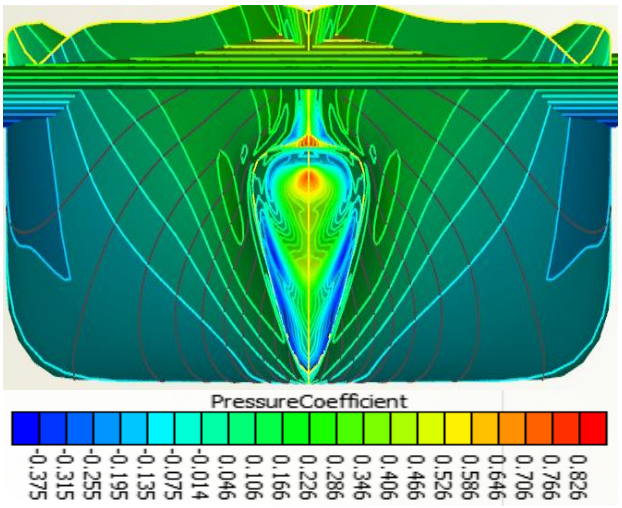

(b) Contour plot of C_P around the bulbous bow for the D3.

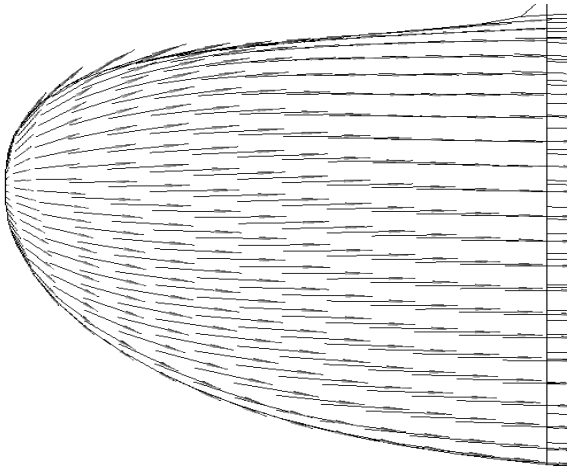

(c) Vector plot of instantaneous velocity around the bulbous bow for the ID.

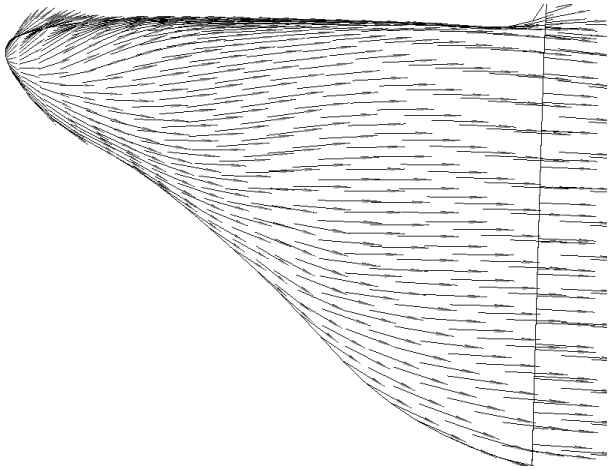

(d) Vector plot of instantaneous velocity around the bulbous bow for the D3.

Figure 24: Plots of C_P contour and instantaneous velocity vectors for the ship around the bulbous bow for ID and D3.

5.4 (d) Additional observations on bulbous bow sections

Because of the reasons mentioned before in Section 2.3 it has only been possible for us to observe and list the simplifications in a qualitative manner rather than a quantitative manner in terms of cost and production complexities. Furthermore, we note here that a bulb with top heavy design (∇) is suitable only for a ship that is expected to run at a constant draft. A significant change in the draft will result into an unfavorable situation in which the majority of the bulb section is out of water (not submerged). This is undesired because it will affect the frictional resistance adversely. Because of this for ships that are expected to operate at significantly varying drafts, a bulbous bow section that has same area of submergence at different drafts is preferable, e.g. O type bulb for oil tanker ships. This analysis is true for bottom heavy design (Δ) also. The Δ and O types when designed with design parameters derived from Figures. 5 to 7 suit a constant draft ship, ideally. Furthermore, we note that a top heavy bulb can have issues related to slamming because of its concentration of area closer to the free surface and less heaviness close to bottom. It can come out of water easily. However, it will have less exposed area to slamming. On this issue, a bottom heavy design is expected to be a better choice. It will not come out of water easily. However, once it come out it be exposed to a large area in slamming. Our focus is on resistance and power and we do not investigate the other parameters that might be of interest to other designers, e.g. slamming, maneuverability, and cost of production etc. These will be explored in the future.

5.5 AFT MODIFICATIONS

After modifications in the forward part of ship, additionally modifications are done in the aft part of ship. As has been explained previously, stern of the KCS is modified after having made changes in the forward part.

Table 9: Computed nominal wake for the different alternatives in stern bulb designs 1 and 2.

Design name	Nominal wake (w_n)	Stern bulb volume (m^3)
Design 3	0.194	114.0
Design 1		
S1-1D3	0.197	166.0
S1-2D3	0.192	169.4
S1-3D3	0.194	230.0
S1-4D3	0.199	326.1
Design 2		
S2-1D3	0.195	104.00
S2-2D3	0.196	100.00
S2-3D3	0.199	94.740
S2-4D3	0.199	91.740

As D3 is showing improvement in the resistance without any significant loss on the propulsive side, this design is explored further with aft modifications. Now, D3 with aft modifications is analyzed again by CFD with Shipflow**TM. Following TM (2014), the nominal wake fraction is:

$$w_n = \frac{(V_s - V_A)}{V} \tag{29}$$

where V_s is ship speed and V_A is the speed of advance. We note that the minimization of bare hull resistance cannot result into minimum power, i.e. minimum drag does not imply minimum power. The thrust deduction - resistance gain due to the presence of propulsor - affects the boundary layer behavior upstream of propulsor and also the pressure distribution on the hull downstream. These two parameters influence the required thrust and power. The wake fraction is important in the efficient design of the propeller to operate properly with the different values of wake fraction across its radial span in between the root and tip. There are two approaches to explore the variation of propulsive efficiency with the wake and they are:

- Analysis of the propeller open water efficiency through Equation (29), and
- Analysis of the hull efficiency which is a function of wake fraction

and they need to be studied in combination. Though, it seems that increasing the w_n can help in minimizing the delivered power, but unfortunately this cannot be considered as an efficient recommended design practice. The increase in w_n can also increase the thrust deduction fraction and therefore the expected improvement in hull efficiency may not occur. Furthermore, the increase in wake fraction can cause an increase in the effective power. Hence, the problem of optimizing a hull shape is more complicated than either minimizing the effective power or maximizing the wake fraction. It needs a detailed study of the flow around hull, flow around propeller and hull-propeller interaction. In the present paper, we have not investigated the above mentioned ideas that demand detailed and focused investigations aiming for the minimum delivered power. This will be investigated by us in future. However, we study the w_n for different stern bulb design alternatives and analyze them to show that the re-designed/modified hull designs do not result into any significant changes in the w_n. And, because there is no significant change in the w_n, we state that the lower resistance will result or translate into the low power. Hence, in our results, an improvement in the resistance also implies an improvement in the delivered power.

5.6 STERN BULB DESIGN 1 OVER FORWARD PART ALREADY MODIFIED (D3)

The aft part – stern bulb – is modified over forward part already modified (Design 3) and the stern bulb performance is studied with CFD (Shipflow**TM). In stern bulb design 1, four designs (S1-1D3, S1-2D3, S1-3D3, and S1-4D3) are generated. The modifications are restricted up to only three ship stations, i.e. AP, St 1, and St 2, mainly because the aim is to modify the ship over a restricted length only. Furthermore, in stern bulb design 1, the stern bulb is basically getting fuller in shape resulting into gain of volume which is advantageous in ship conversion/modification. The nominal wake on propeller disk is computed for each design to study the propulsive performance of propeller. The C_T values, bulb volume and nominal wake for each of the design alternatives are listed in Figure 25k and Table 9. From Figure. 25k, amongst all the designs (S1-1D3, S1-2D3, S1-3D3, and S1-4D3), the design S1-2D3 shows a better performance because of lower C_T value. However, the design S1-2D3 has a higher C_T value as compared to the design D3 (i.e. Design 3 without any aft modification). The nominal wake contours are shown in Figure. 25a to 25f for all the design alternatives. From these figures, amongst all the designs (S1-1D3, S1-2D3, S1-3D3, and S1-4D3), there is no significant change in the nominal wake. However, at the marginal level, the nominal wake is lowest for the design S1-2D3 and also the nominal wake contours are smoothest for this design.

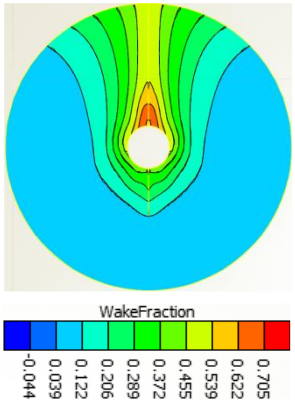

(a) Contour plots of the nominal wake on the propeller disk for ID.

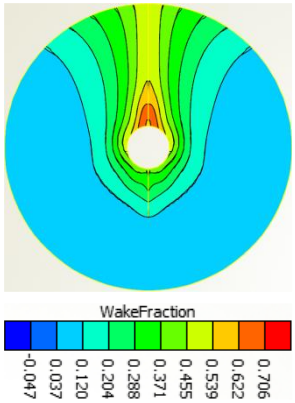

(b) Contour plots of the nominal wake on the propeller disk for D3.

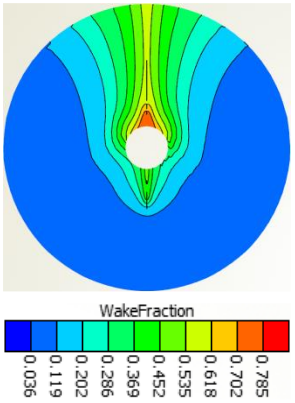

(c) Contour plots of the nominal wake on the propeller disk for S1-1D3.

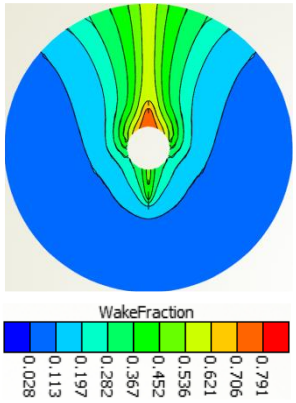

(d) Contour plots of the nominal wake on the propeller disk for S1-2D3.

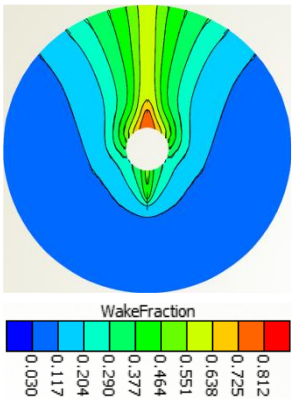

(e) Contour plots of the nominal wake on the propeller disk for S1-3D3.

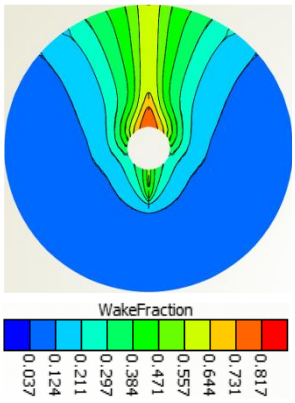

(f) Contour plots of the nominal wake on the propeller disk for S1-4D3.

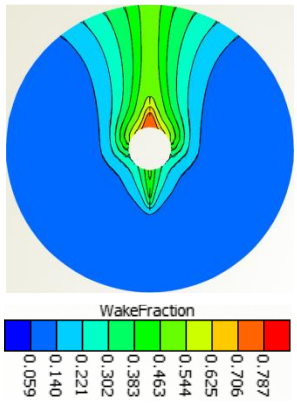

(g) Contour plots of the nominal wake on the propeller disk for S2-1D3.

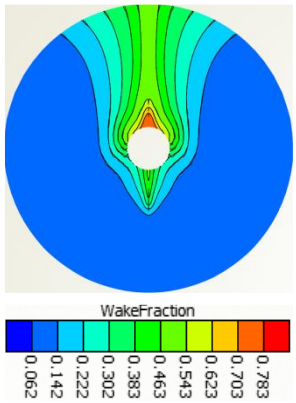

(h) Contour plots of the nominal wake on the propeller disk for S2-2D3.

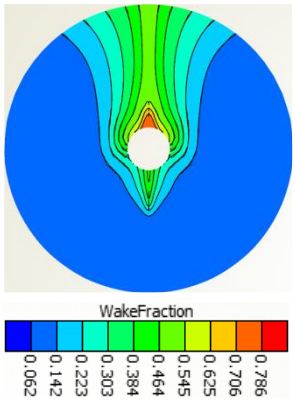

(i) Contour plots of the nominal wake on the propeller disk for S2-3D3.

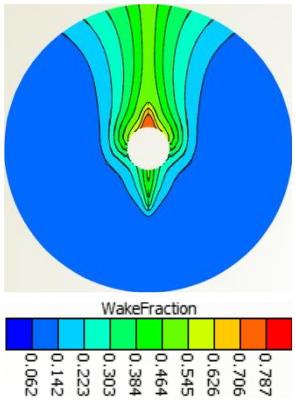

(j) Contour plots of the nominal wake on the propeller disk for S2-4D3.

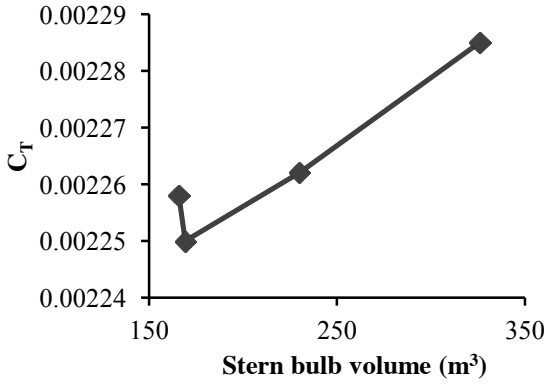

(k) Computed C_T values for the different alternatives in stern bulb design 1.

Figure 25: Contour plots of the nominal wake on the propeller disk for ID, D3, S1-1D3, S1-2D3, S1-3D3, S1-4D3, S2-1D3, S2-2D3, S2-3D3 and S2-4D3; and computed CT values for the different alternatives in stern bulb design 1.

5.7 STERN BULB DESIGN 2 OVER FORWARD PART ALREADY MODIFIED (D3)

In second design approach, the aft part – stern bulb – is modified over forward part already modified (D3) and the stern bulb performance is studied with CFD (Shipflow[**TM]). In stern bulb design 2, four designs (S2-1D3, S2-2D3, S2-3D3, and S2-4D3) are generated. The modifications are restricted up to only three ship stations, i.e. AP, St 1, and St 2, mainly because the aim is to modify the ship over a restricted length only. Furthermore, in stern bulb design 2, the stern bulb is basically getting finer in shape resulting into loss of volume which can advantageous in extracting a better flow around propeller. The nominal wake on propeller disk is computed for each design to study the propulsive performance of propeller. The C_T values, bulb volume and nominal wake for each of the design alternatives are listed in Figure 25g, 25h, 25i and 25j, 26a and Table 9. From these figures, amongst all the designs (S2-1D3, S2-2D3, S2-3D3, and S2-4D3), the design S2-4D3 shows a better performance because of lower C_T value. From, Figure. 26a, however, still, the design S2-4D3 has a higher C_T value as compared to the design D3 (i.e. Design 3 without any aft modification). The nominal wake contours are shown in Figure. 25 for all the design alternatives. From Figure. 25g to 25j, amongst all the designs (S2-1D3, S2-2D3, S2-3D3, and S2-4D3), there is no significant change in the nominal wake. However, at the marginal level, the nominal wake is lowest for the design S2-1D3 and also the nominal wake contours are smoothest for this design.

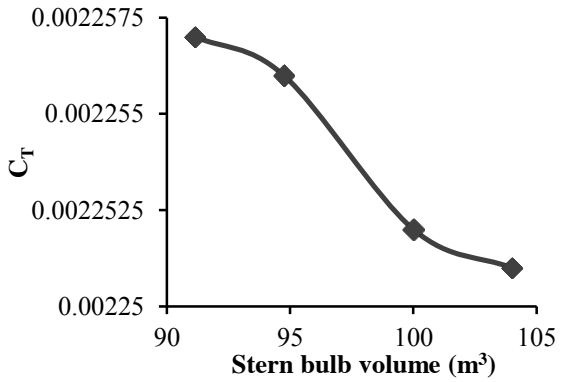

(a) Computed C_T values for the different alternatives in stern bulb design 2.

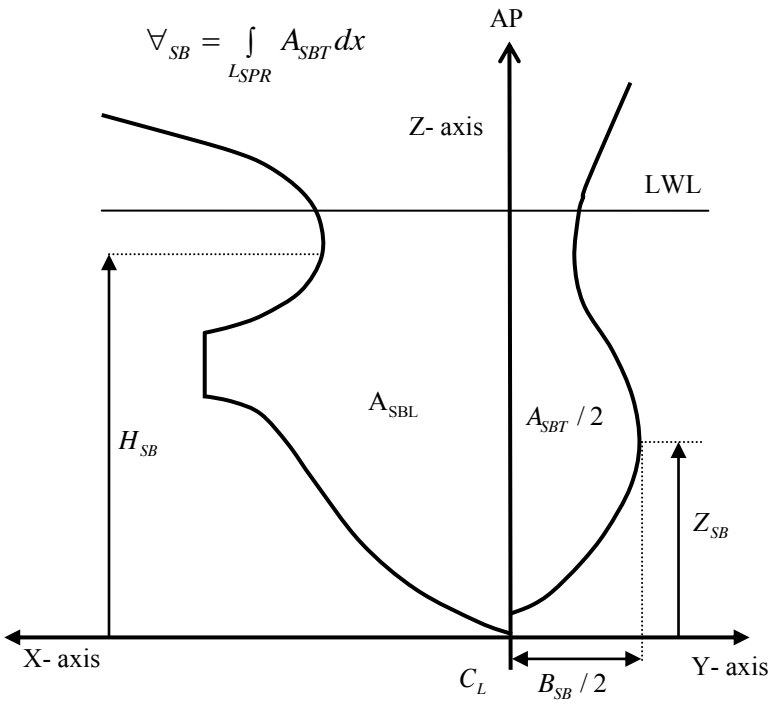

(b) Description of the stern bulb parameters.

Figure 26: Computed C_T values for the different alternatives in stern bulb design 2 and description of stern bulb parameters.

5.8 COMPARATIVE STUDY OF THE CURRENT RESEARCH WITH PREVIOUS RESEARCHES

A comparative study of the current research with previous researches is reported in Table 10. As per the best of our knowledge, for similar application, no existing research has reported a gain in resistance that is significantly higher than our results and no analysis has been reported that deals with the production costs related to modified/re-designed ship.

It is difficult, if not impossible, to get a reliable data on ship production/repair costs and it is because shipyards are reluctant to share their cost structures. Furthermore, the cost structures of ship production and repair are dominated by extraneous factors also and they are beyond the control of shipyard. However, a qualitative analysis can be tried for the production costs. And, in the previous sections, we reported a qualitative analysis related to production cost and adopted design strategies that are aimed towards the less cost of production. Also, within the constant cost life-cycle analysis, it is well known that lower resistance results

Table 10: Comparative study of the current research with previous researches.

S. No.	Reference	Details about the 'Ship – Original (SO)' and 'Ship - Optimized/re-designed (SR)'	Range of F_n	Maximum reported reduction	Critical analysis
1	Campana et al. (2006)	Model 5415 from Stern et al. (2000) SO and SR both with bow and sonar dome	0.280	3.80% in the total resistance	- No design approach reported related to basic ship parameters. Hence, results are difficult to reproduce across a range of applications. - No analysis of gain in the resistance to the gain in power, whether it will be possible or not? - No consideration for the production constraints in the design of sectional shapes. - No comment about the manufacturing cost.
2	Tahara et al. (2008)	Model 5415 B from Stern et al. (2000) SO and SR both with bow and sonar dome	0.280	3.90% in the total resistance	- do -
3	Kim and Yang (2010)	KRISO container ship (KCS) SO and SR both with bulbous bow	0.220	3.6 % in the total resistance	- do -
4	Park et al. (2015)	KSUEZMAX ship SO and SR both with bulbous bow	0.162	2.4 % in the total resistance	- do -
5	Huang and Yang (2016)	Series 60 ship SO without bulbous bow and SR with bulbous bow	0.270	6.42% in the total resistance	- do -
6	Our current research	KRISO container ship (KCS) SO and SR both with bulbous bow	0.255	3.50 % in the total resistance	- Design approach is related to basic ship particulars and hence, results are easy to reproduce across a range of applications. - Design curves are reported for the C_B = 0.650, 0.675, 0.700, and 0.725 across the F_n = 0.26 – 0.30. - A critical analysis of resistance to power is reported. - Production constraints are considered in the design of sectional shapes. - No comment about the manufacturing cost.

in: drop in fuel consumption, increase in speed range and increase in maximum operating speed. With less resistance and favorable nominal wake fraction, the propeller cavitation characteristics will improve considerably. Furthermore, the enhanced volume, space, and area provided by the modified bulb and stern may be utilized to house additional systems, for more details see Cusanelli (1994). Hence, the detailed design and analysis approach presented here advances and deepens the currently available design and modification strategies for the ships.

6. CONCLUSIONS

We have presented a re-design/modification formulation that can be applied to concept design or existing design modifications, e.g. conversion of containership into tanker. From the presented results, we can draw the following conclusions:

- We have presented a design method for bulbous bows for ships in the range C_B = 0.650 - 0.725 and F_n = 0.260 - 0.300 along with a detailed CFD driven approach for the hydrodynamic analysis integrated with CAD.
- The results of Figures. 5 to 7 are applicable to the design of ships with bulbous bows and these can be used by any shipyard or ship designer.
- All the developed designs have been reported with some of the important lines drawings and these can be checked for confirming their applicability.
- An integrated design model has been presented for ship hull form modification. Alternate design solutions have been generated and studied using NAPA*TM and Shipflow**TM. The design solutions have been evaluated by a procedure incorporating the V&V methodology of ITTC. The presented approach is applicable to different types of ships in the ranges mentioned above and these ranges cover a large group of commercial ships.
- The design modifications have been done by modifying both aft and forward part of the ship. And different design alternatives are provided for both forward and aft modifications. Furthermore, the earlier work of Sharma and Sha (2005b) has been extended. The bulbous bow (forward modifications) design parameters have been derived for the C_B = 0.650, 0.675, 0.700, and 0.725 across the F_n = 0.26 – 0.30. And design process has been demonstrated for commercial ship of C_B = 0.65 at the design speed of V_S = 24 knots.
- Each of the candidate designs has been evaluated for resistance, nominal wake study, and different range of speed around the V_S = 24 knots. Following the design modifications, volume gains in each of the design modifications are also calculated to add the knowledge of possible design modifications.
- In forward bulb modifications, design modifications have shown the improvement in the C_w and C_T values. Overall, in forward design modifications, Design 3 gives the improvement in C_w and C_T value by 10% and 3.50% respectively than the initial design. Gain in volumes for Design 1, Design 2, and Design 3 are 453.70 m^3, 221.00 m^3, and 194.00 m^3 respectively. Finally, in the aft modification, effect of stern bulb has been analyzed by evaluating the nominal wake at the propeller plane. And, it has been shown that the gains reported in the resistance are not lost on the propulsive side.
- From the ship hull form design point of view the transitions modules TMFBMB and TMABMB are important because they allow smooth fairing of the fore body to middle body and the aft body to middle body, e.g. ensure that no hard shoulders exist. The problem of hard shoulder is important in ships of high bilge radius, i.e. a high bilge radius demands longer length of transition zones to ensure smooth merging of the middle body with the fore and aft bodies. Additionally, the waves generated by different parts of the ship show variations in the amplitude and phase difference depending upon the geometry (i.e. volume, shape and their distribution) of the part, i.e. volume largely affect the amplitude and shape variation affects the phase difference. Primarily, the transition modules will affect the phase difference but their influence will be less as compared to the effects of bulbous stern and bow. Herein, we have not focused on the transition modules. However, as these modules have very specific application and importance (i.e. in ships with high bilge radius when there are difficulties in merging the forward and aft-body modules with the mid-body module), we shall explore them in our future research.
- However, in our approach, the stern bulb has been re-designed from the experience gained from literature survey (Bessho (1967), Suzuki *et al*. (2005)). The presented approach is manual and does not allow automatic generation of stern bulb and integrated analysis with CAD and CFD. Furthermore, the stern bulb parameters have not been derived as methodically as the bulbous bow design parameters. E.g. using the idea of bulbous bow design parameters, stern bulb parameters can be defined as shown in Figure. 26b. And, in future the aim will be to derive the design parameters of Figure. 26b.
- The final decision in ship re-design and modification is governed by multiple considerations, e.g. production, structural and hydrodynamic. Our present work focused only on the improvements in the resistance and power and we did not focus on other aspects. An improvement in resistance and power will result into significant savings. However, a modification will also cost monetarily in terms of costs related to the production. So, the issue will become cost/benefit analysis between the cost of

production and the benefit of lower resistance and power. A final decision will be taken after a thorough cost and benefit analysis and that is specific to the ship, ship builder and other issues. In future, we shall aim for an extension of the present approach to include the detailed analyses integrating hydrodynamics with production and structures.

Also, the presented approach for re-design/modification is integrated in a sense that the CAD model of NAPA*TM is compatible with Shipflow**TM and the modified designs in NAPA*TM can be analyzed in Shipflow**TM without any interface. This is restricted and limited integration because there is no automatic loop in which the design can be automatically generated with basic values of the design parameters. This loop will demand the enhanced geometric modeling capabilities and some iterative procedure to achieve desired shapes. This needs to be explored in future.

Our future works will go in the above mentioned directions and currently these are under investigation.

7. COPYRIGHTS AND TRADEMARKS

*Trademark and copyright with ClassNK (Nippon Kaiji Kyokai), Japan; **Trademark and copyright with Flowtech Inc., Sweden.

8. ACKNOWLEDGEMENTS

This research was supported by the internal research grants of the IIT Madras, Chennai, India via a scholarship grant scheme: OE10S024.

9. REFERENCES

1. ASANO, S. (1979). *A consideration on the energy of secondary flow around a ship section* (in Japanese). Journal of the Kansai Society of Naval Architects of Japan, 174, 69–75.
2. BESSHO, M. (1967). *Study into frame-line configuration* (in Japanese). Journal of the Society of Naval Architects of Japan, 122, 43–65.
3. CAMPANA E. F., D. PERI, Y. TAHARA, and F. STERN (2006). *Shape optimization in ship hydrodynamics using computational fluid dynamics*. Computer Methods in Applied Mechanics and Engineering, 196 (1–3), pp. 634-651.
4. CAMPANA, E. F., G. LIUZZI, S. LUCIDI, D. PERI, V. PICCIALLI and A. PINTO (2009). *New global optimization methods for ship design problems*. Optimization and Engineering, 10, pp. 533–555, DOI: 10.1007/s11081-009-9085-3.
5. CHEN, J., J. WEI, and W. JIANG (2016). *Optimization of a twin-skeg container vessel by parametric design and CFD simulations*. International Journal of Naval Architecture and Ocean Engineering, 8, pp. 466-474.
6. COTTRELL J. A., T.J.R. HUGHES, and Y. BAZILEVS (2009). *Isogeometric Analysis: Toward Integration of CAD and FEA*, Wiley, USA, 1st edition.
7. CUSANELLI D. S. (1994). *Development of a bow for a naval surface combatant which combines a hydrodynamic bulb and a sonar dome*", in American Society of Naval Engineers Technical Innovation Symposium, pp.231 - 247.
8. ITTC (2008). *General uncertainty analysis in CFD verification and validation methodology and procedures*. Recommended Procedures and Guidelines, 7.5-03-01-01.
9. HUANG F. and C. YANG (2016). *Hull form optimization of a cargo ship for reduced drag*. *Journal of Hydrodynamics*, 28 (2), pp. 173-183.
10. HUGHES, T.J.R., J.A. COTTRELL, and Y. BAZILEVS (2005). *Isogeometric analysis: CAD, finite elements, NURBS, exact geometry and mesh refinement*, Computer Methods in Applied Mechanics and Engineering, 194, Issues 39-41, 4135–4195.
11. KIM H. and C. YANG (2010). *A new surface modification approach for CFD-based hull form optimization*. Journal of Hydrodynamics, 22 (5), Supplement, pp. 520-525.
12. KOSTAS, K. V., A. I. GINNIS, C. G. POLITIS, and P. D. KAKLIS (2015). *Ship-hull shape optimization with a T-spline based BEM–isogeometric solver*. Computer Methods in Applied Mechanics and Engineering, 284, pp. 611–622.
13. KRACHT, A.M. (1978). Design of bulbous bows, *Transactions SNAME*, 86,197-217.
14. MISRA, S. C. (2015). *Design Principles of Ships and Marine Structures*, 1st edition, CRC Press, USA.
15. MISRA S.C., O.P. SHA, and R.P. GOKARN (2002). *Modularized ship designs for competitive construction in India*. SNAME Transactions, 110, 279-299.
16. MICHELL, J. H. (1898). *The Wave Resistance of a Ship Moving*, Philosophical Magazine, vol. 45, pp. 106 - 116.
17. NMRI (2014). KRISO Container Ship (KCS), website address: www.nmri.go.jp/institutes/fluid_performance_evaluation/cfd_rd/cfdws05/gothenburg2000/KCS/kcs_format.htm
18. NOWACKI, H. (2010). *Five decades of Computer-Aided Ship Design*. Computer-Aided Design, 42, pp. 956-969.
19. NOWACKI, H. and M.I.G BLOOR (1995). *Computational Geometry for Ships*, World Scientific, Singapore.

20. PAPANIKOLAOU, A. (2010). *Holistic ship design optimization*. Computer-Aided Design, 42, pp. 1028-1044.
21. PARK J.-H., J.-E. CHOI and H.-H. CHUN (2015). *Hull-form optimization of KSUEZMAX to enhance resistance performance*. International Journal of Naval Architecture and Ocean Engineering, 7, pp. 100-114.
22. PATEL, A. K. P. (2016). *Development of an Integrated Design Model for Ship Hull Form Modification*, Master of Science (By Research) Thesis, Department of Ocean Engineering, IIT Madras, Chennai, India.
23. PATRIKALAKIS, N. M. and T. MAEKAWA (2002) *Shape Interrogation for Computer Aided Design and Manufacturing*, Springer, Germany.
24. SAPIDIS, N. S. (1987) *Designing Fair Curves and Surfaces: Shape Quality in Geometric Modeling and Computer-Aided Design*, SIAM, USA.
25. SERANI, A., M. DIEZ, C. LEOTARDI, D. PERI, G. FASANO, U. IEMMA, E. F. CAMPANA (2014). *On the use of synchronous and asynchronous single-objective deterministic particle swarm optimization in ship design problems*. In the Proceedings of International Conference on Engineering and Applied Sciences Optimization 2014, Editors: M. Papadrakakis, M. G. Karlaftis, and N. D. Lagaros, Kos Island, Greece, 4-6, June 2014, pp. 1-23.
26. SHA, O.P., S.C. MISRA, and R.P. GOKARN (2004). *Ship hull form design – A modular approach*, In: Proceedings on 9th Symposium on Practical Design of Ships and Other Floating Structures (PRADS - 2004), Luebeck - Travemuende, Germany, 1-8.
27. SHARMA, R., and O. P. SHA (2005a). *Hydrodynamic Design of Integrated Bulbous Bow / Sonar Dome for Naval Ships*. Defence Science Journal, 55 (1), pp. 21 – 36.
28. SHARMA, R., and O.P. SHA (2005b). *Practical Hydrodynamic Design of Bulbous Bows for Ships*. Naval Engineers Journal, 117(1), 57-76.
29. SHARMA, R. and O.P. SHA (2007). *Development of an ERP model for modularly designed ships for medium scale shipyards – I: Manufacturing Management*. Journal of Marine Engineering and Technology, No. A10, 17-43.
30. SHARMA, R. and K. TAE-WAN (2010). *Development of a logic-based product life-cycle management (LBPLM) system for shipbuilding industry - conceptual development*. Journal of Ship Production and Design (JSPD), 26 (4), 231 - 251.
31. STERN F., J. LONGO, R. PENNA, A. OLIVIERI, T. RATCLIFFE and H. W. COLEMAN (2000). *International collaboration on benchmark CFD validation data for surface combatant DTMB model 5415*. In the Proceedings of 23rd Symposium on Naval Hydrodynamics, Val de Ruil, France, pp. 213-24.
32. SUZUKI, K., H. KAI and S. KASHIWABARA (2005). *Studies on the optimization of stern hull form based on a potential flow solver*. Journal of Marine Science and Technology, 10, 61–69.
33. TAHARA Y., D. PERI, E. F. CAMPANA and F. STERN (2008). *Computational fluid dynamics-based multiobjective optimization of a surface combatant using a global optimization method*. Journal of Marine Science and Technology, 13, pp. 95-116.
34. TM (2014). SHIPFLOW Version 5.1- user's manual. FLOWTECH Int. AB, Gothenburg, Sweden.
35. YANG, C., and F. HUANG (2016). *An overview of simulation-based hydrodynamic design of ship hull forms*. Journal of Hydrodynamics, 28 (6), pp. 947-960, DOI: 10.1016/S1001-6058(16)60696-0.
36. YIM, B. (1980). *Simple calculation of sheltering effect on ship-wave resistance and bulbous bow design*. Journal of Ship Research, 24 (4), 232 - 243.
37. YIM, B. (1974). *A Simple Design Theory and Method for Bulbous Bows of Ships*, Journal of Ship Research, vol. 18, no. 3, pp. 141 - 152.

